



Large area diamond detectors as heavy ion beam profilers

Marian PARLOG

Laboratoire de Physique Corpusculaire de Caen

HIE ISOLDE Technical Workshop
The 28th-29th of November 2013



I Introduction:

- *Goal and framework: beam profilers – EURISOL, SPIRAL2, SPARC... & focal plane of the associated spectrometers*

II The synthetic diamond: (*properties, fabrication, principle of detection*)

- *Single-crystal (sc-CVD) and polycrystalline (pc-CVD) sensors*
- *Response and charge collection = f(material quality & thickness, ion Z&E, U)*

III Non-segmented detectors:

- *Construction at LPC and test at GSI (classical electronics) and GANIL (sampling)*
- *Stability of the signal in time; pulse shape analysis (PSA)*

IV Double-sided multi-strip detectors:

- *construction at LPC and tests at GANIL (PSA); analysis in progress*

V Conclusions and prospective

II Diamond properties:

Excellent radiation hardness due to:

- the highest thermal conductivity
- the high energy of 80 eV to remove an ion

No p-n junction is required:

- due to the large band gap;
- simply metallic electrodes (like an ionization chamber);

High electric fields, up to 6 V/ μm :

- due to the high resistivity;
- small dark current (negligible intrinsic carrier concentration at room temperature)

Narrow pulses, due to:

- the low capacitance;
- the high carrier mobility;

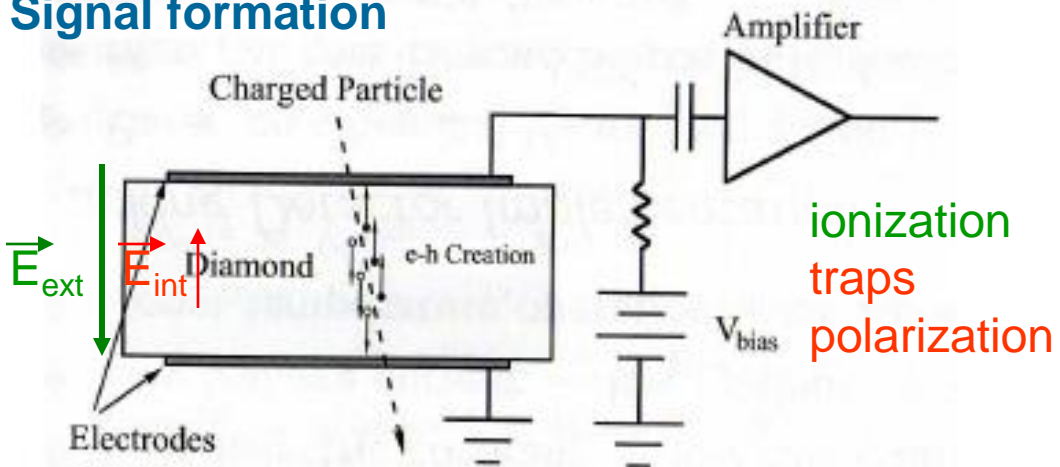
CVD diamonds:

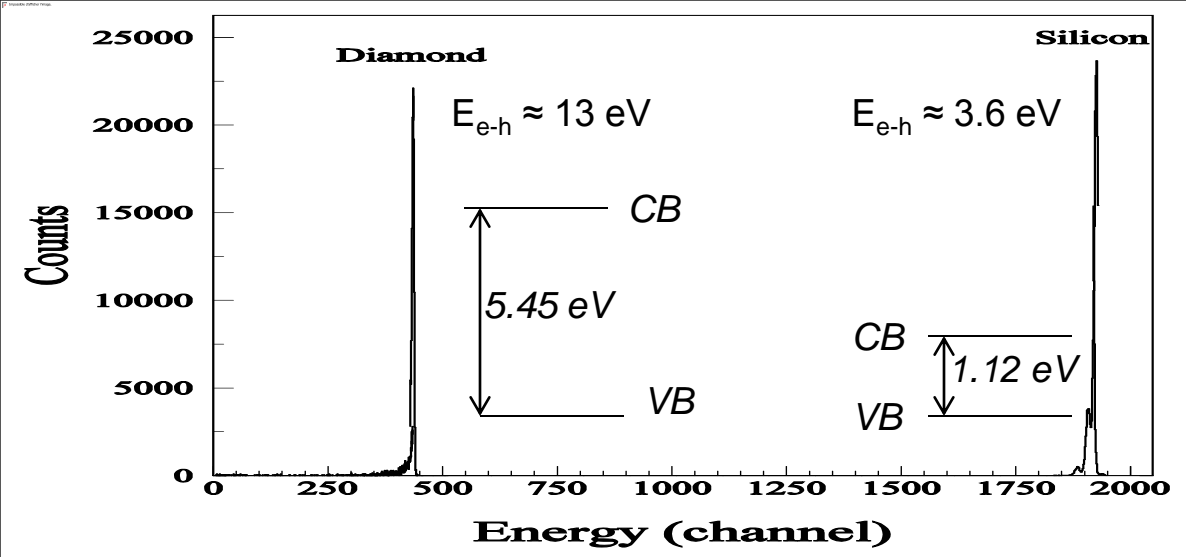
allow big detector areas, can be metalized with any desired shape, can be wire bonded, can be operated as « noise-free » particle counter

Tab. 1. Physical Properties of Diamond and Silicon

Physical properties at 300K	Diamond	Silicon
Band Gap (eV)	5,45	1,12
Electron mobility (cm ² /Vs)	1800-2200 ?	1500
Hole mobility (cm ² /Vs)	1600-2400 ?	600
Resistivity ρ ($\Omega \cdot \text{cm}$)	$>10^{11}$	$2,3 \cdot 10^5$
Dielectric constant ϵ_r	5,7	11,9
Thermal conductivity (W/cm.K)	20	1,27
Lattice constant (Å)	3,57	5,43
Energy to remove an atom from the lattice (eV)	80	28
Energy to create a pair e-h (ev)	13	3,6

Signal formation

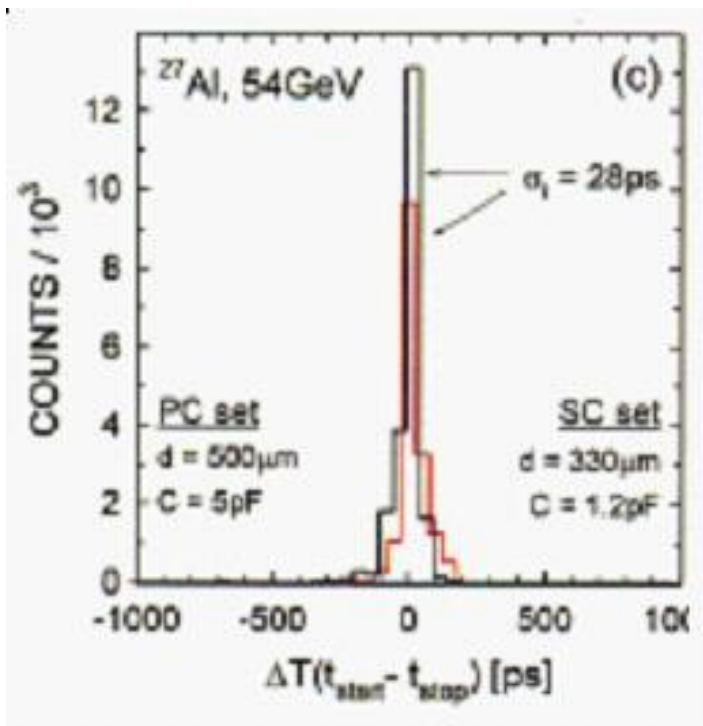




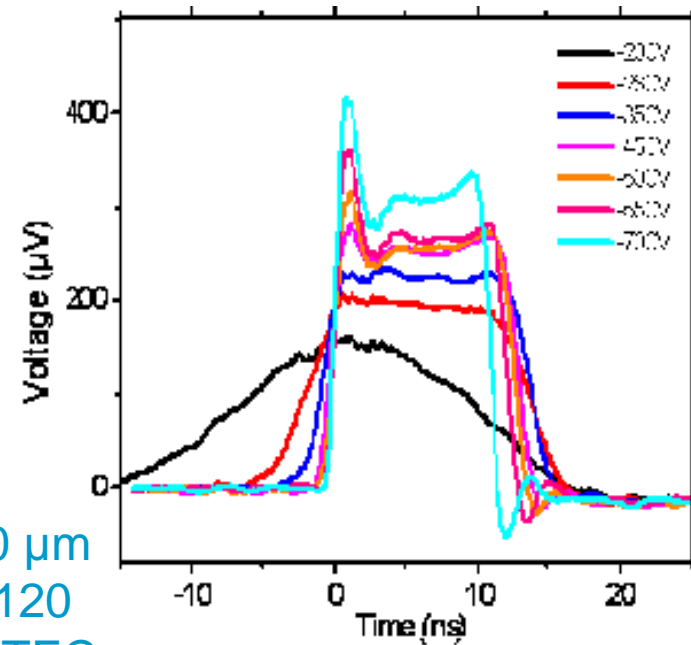
The CVD diamond detectors may behave in very different ways:
Single-crystal diamond
detector (CEA Saclay) of $20 \mu\text{m}$ thickness, adapted to the range.
(courtesy of J.-L. Lecouey –LPC)

The signal is 4 lower (left peak) than in a Si detector (right)

$^{241}\text{Am}: \alpha$ of 5.5MeV
Range $\sim 15 \mu\text{m}$



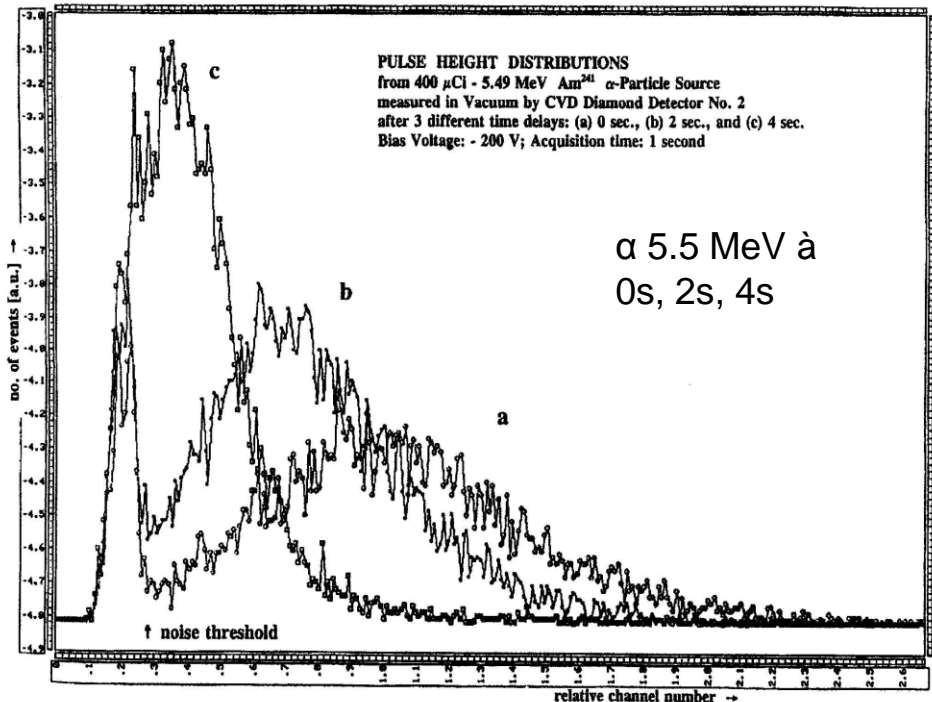
GSI:
Signals &
TOFE.
Berdermann
for the
NoRH Dia
collaboration



II. Synthetic Diamond

courtesy of Dr. H. Hamrita, LIST – CEA Saclay

II. D i a m o n d



The CVD diamond detectors may behave in very different ways:

Polycrystalline-crystal diamond drawback:
the bulk polarization
Solutions:

- Previous radiation;
- Subbandgap light;
- Electronic procedure;
- Thermic procedure
- **Good material!!!**

the salutary solution

Requirements for a (radioactive) beam profiler working below 10^6 pps:

- The beam profile (X,Y) - resolution of 1mm over an active area of up to $50 \times 50 \text{ mm}^2$.
- The device should operate at beam intensities as low as ~ 1 pps and up to $\sim 10^6$ pps.
- The detector should exhibit a fast rise time for timing applications (TOF ~ 0.5 ns) as well as a short response time to enable operation at ~ 1000000 pps.
- The detector should have a large dynamic range – both very light and very heavy ions with energies ranging from a few to ~ 250 MeV/nucleon should be detectable.
- The detectors should be robust and radiation hard so as to reduce to a minimum their replacement or removal for repair.
- Provide for an accurate and precise measurement of the intensity.
- For safety reasons the detector must have a good vacuum integrity.
- **Insensitive to the decay of the radioactive ions** (ie., e⁻, e⁺, g⁺, etc.).

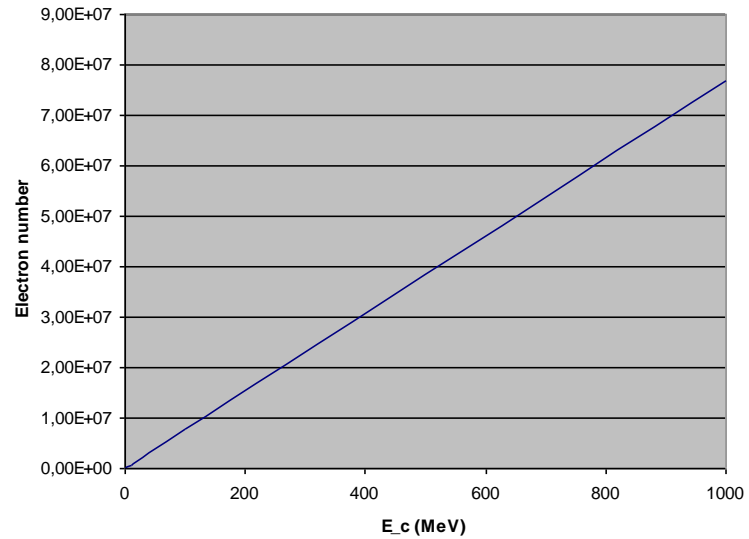
From a practical point of view (eg, use by operators during beam tuning) the detectors should be as simple and straightforward to operate as possible.

Alternative: the large area synthetic polycrystalline diamond (chemical vapour deposition – CVD), have properties matching very closely those needed to fulfil the above requirements (**R&D SPIRAL2 in LPC and SPARC Task 4.1 at FAIR**)

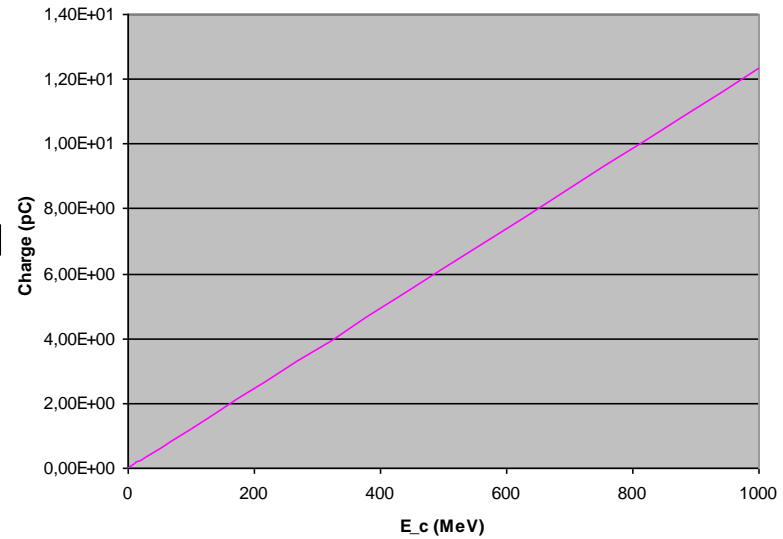
Electron number

1 MeV => 77000 e- => 12.3 fC

Charge (pC)

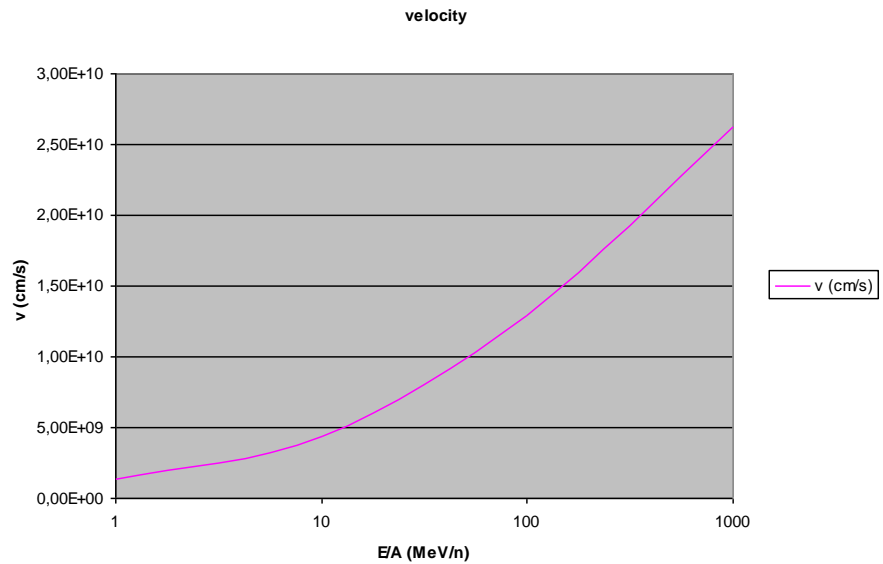


electron number



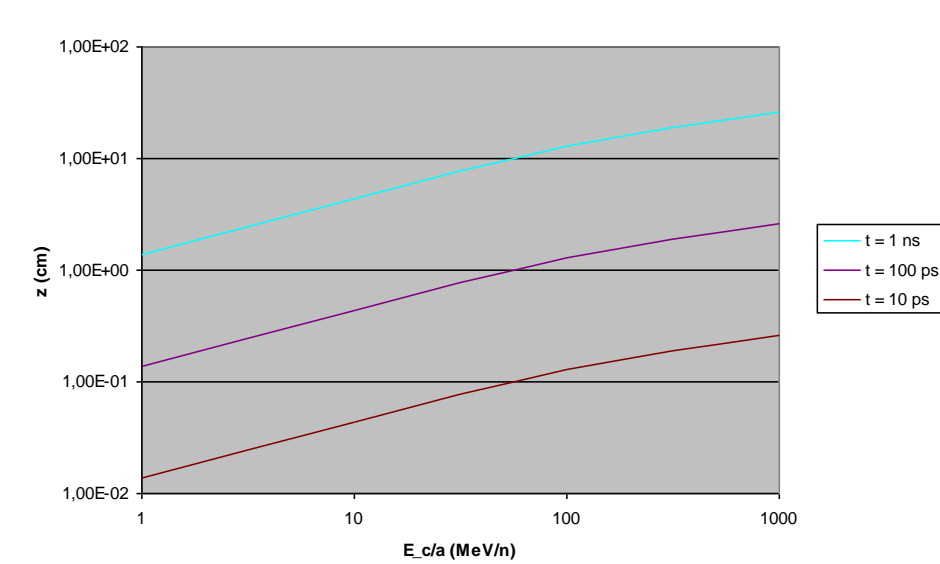
Charge (pC)

velocity



v (cm/s)

spatial resolution

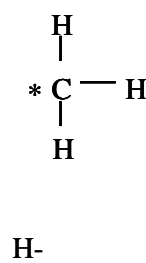
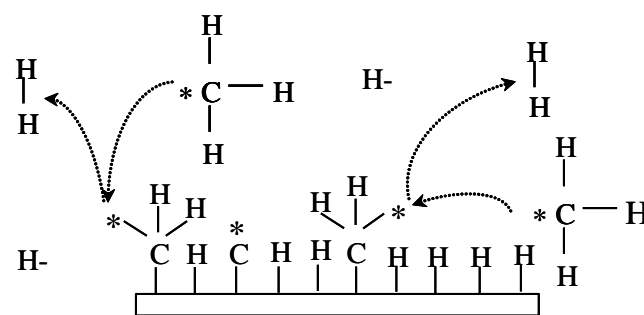
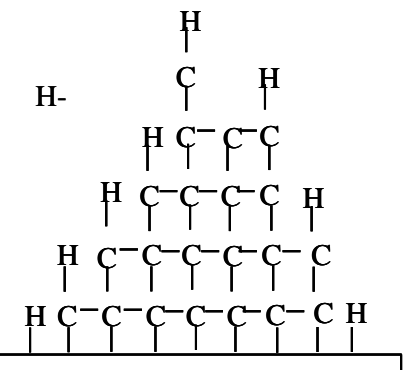
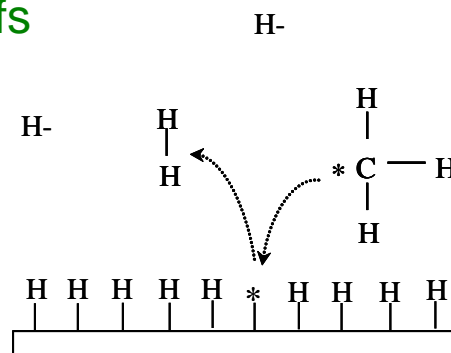


- $t = 1$ ns
- $t = 100$ ps
- $t = 10$ ps

Croissance du diamant Chemical Vapor Deposited (CVD)

Synthèse à partir du méthane CH_4 et d'hydrogène H_2

Réaction des atomes d'hydrogène avec la surface, création de sites actifs



Extraction d'hydrogène

Liaison des atomes de carbone avec leurs voisins : formation du cristal du diamant

III Not-segmented detectors: polycrystalline diamond

Cleaning: eau régale + ultra-sounds

($1/5 \text{ H}_2\text{O} + 3/5 \text{ HCl} + 1/5 \text{ HNO}_3$)

Electrodes: Au (ageing) or Al;

if not: CrAu, NiAu, TiPtAu)

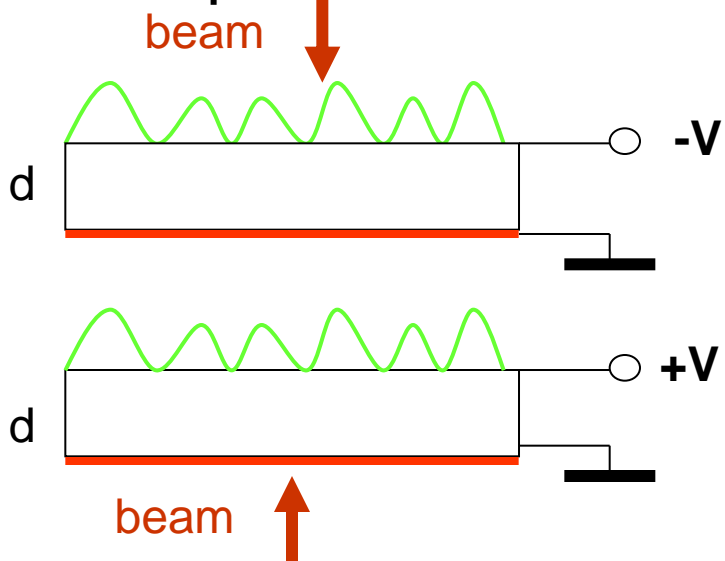
Contacts: bonding

(Al wire – soldering T + ultra-sounds)

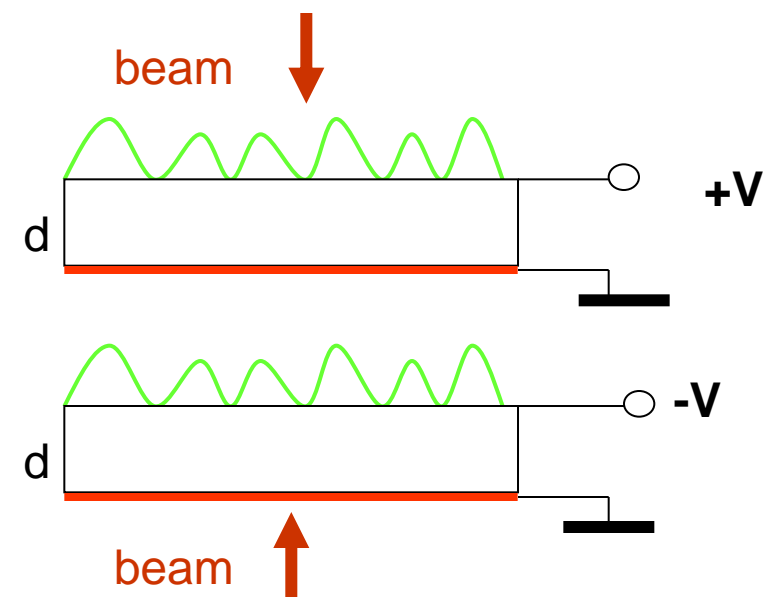
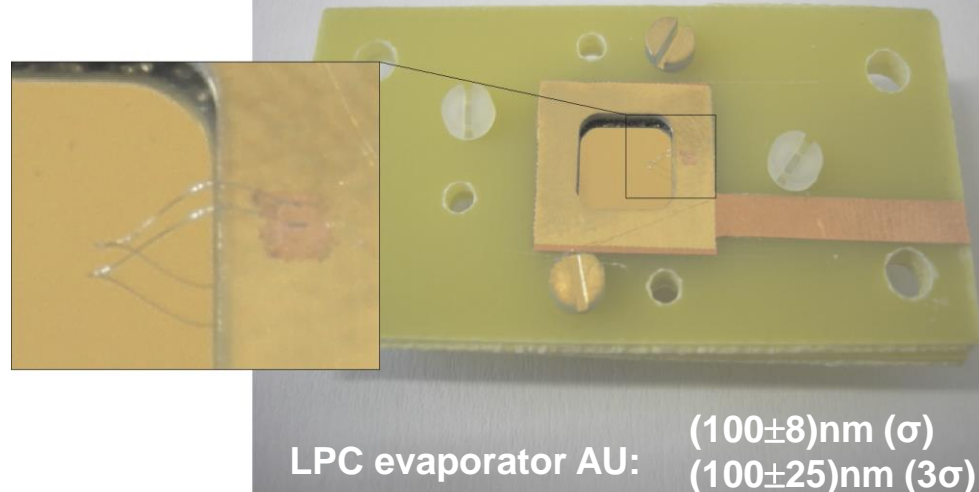
Voltage: $\pm 1\text{V}/\mu$ or higher

Irradiation: growth face or nucleation face

– to be compared



Range $<< d$: transit electrons



Range $<< d$: transit holes

III Not-segmented detectors: polycrystalline diamond



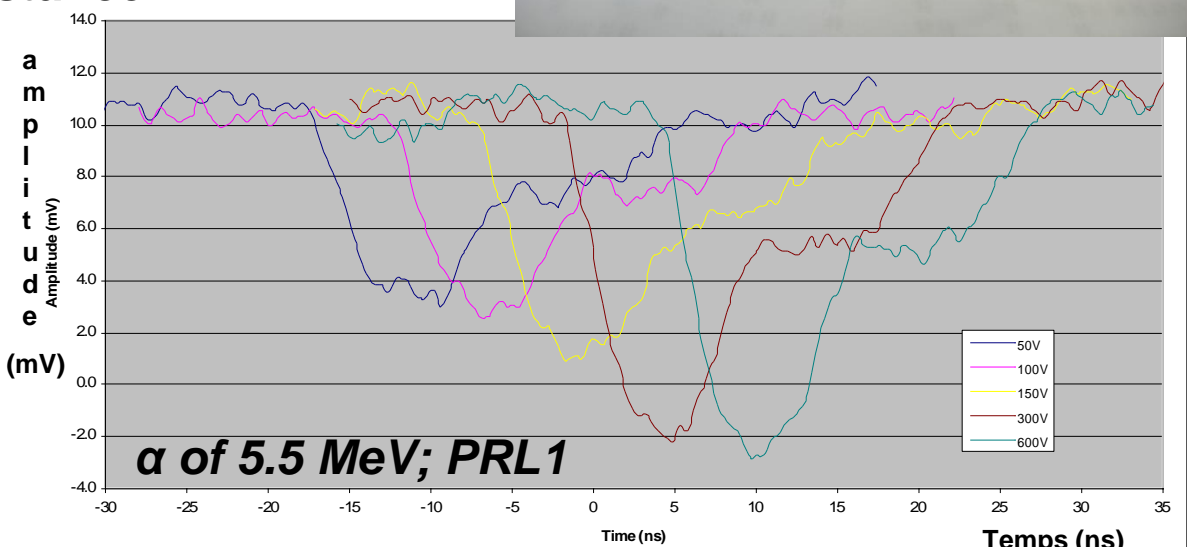
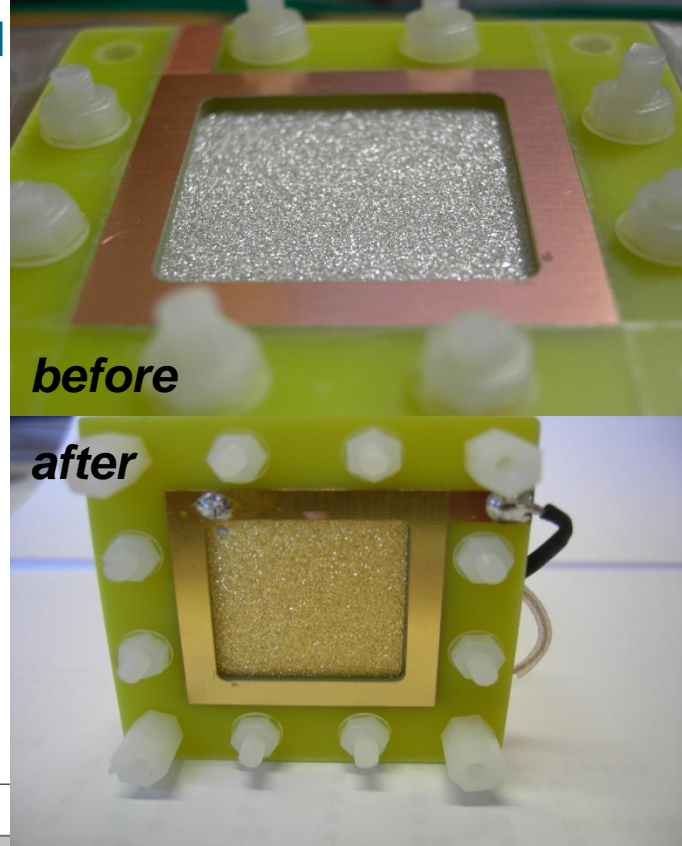
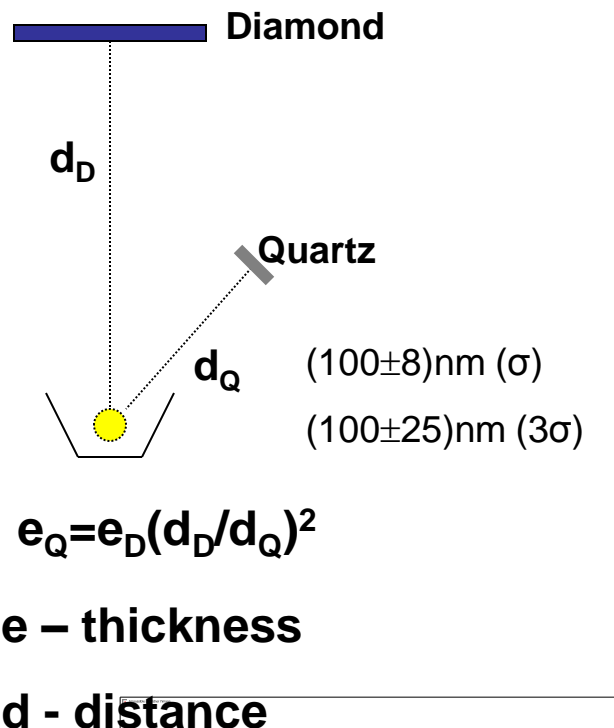
The LPC evaporator

Incomplete collection of charge carriers: when the HV increases, the amplitude increases, the collection being improved

Company 1:

det1: P1N ELA (as grown) 300 μ

det2: P2 ELP 500 μ



Amplitude variation of signals - different voltages HV

Tests of not-segmented detectors in HI beams

Electronics &

Acquisition:

GSI:

- classical

GANIL:

- MATACQ – VME

(400 MHz BW -> 0,9ns;

2GHz sampling)

- oscillo LeCroy 64Xi

(600 MHz BW -> 0,6ns;

10Gs/s)

det1 **Comp1 P1N ELA** 300 μm

det2 **Comp1 P2 ELP** 500 μm

det3 **Company 2** 630 μm

det4 **Company 2** 200 μm

det5 **Company 3**
165 μm
det6 100 μm
det7 70 μm
& a 500 μ sc tested in 6AMeV 238U beam

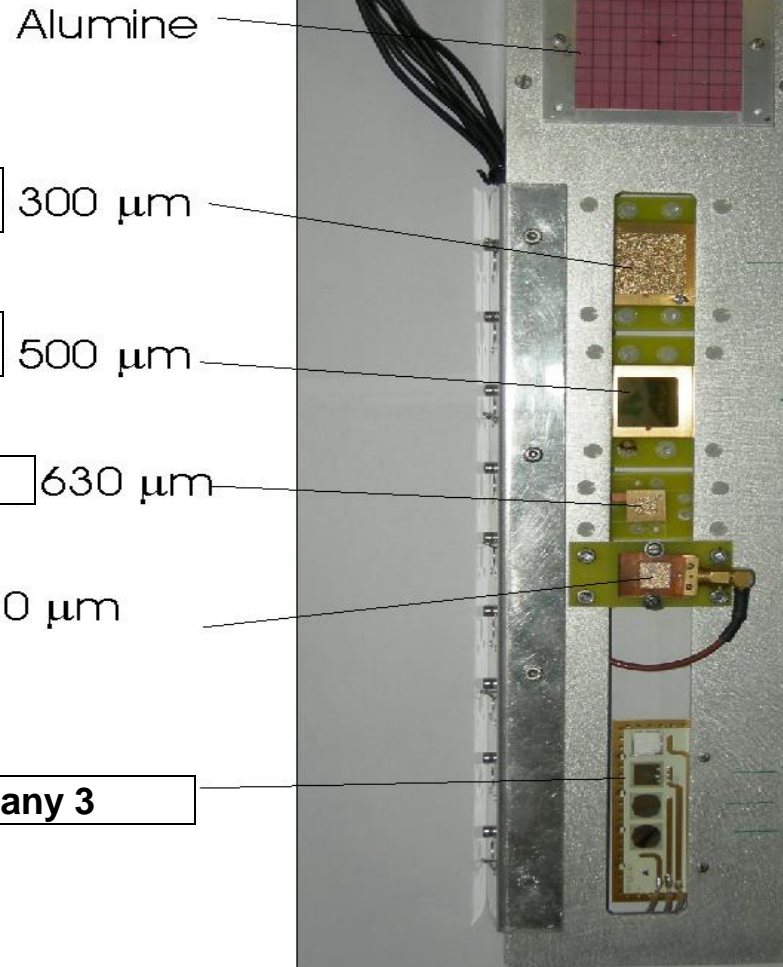
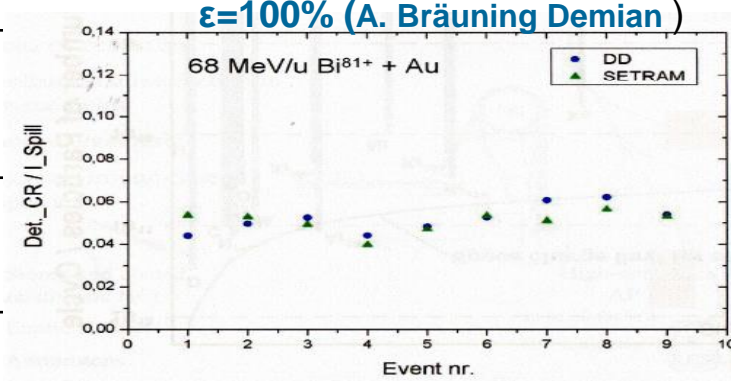


Table 2. Energy per nucleon and range of the ions which have served to test the uni-strip diamond detectors.

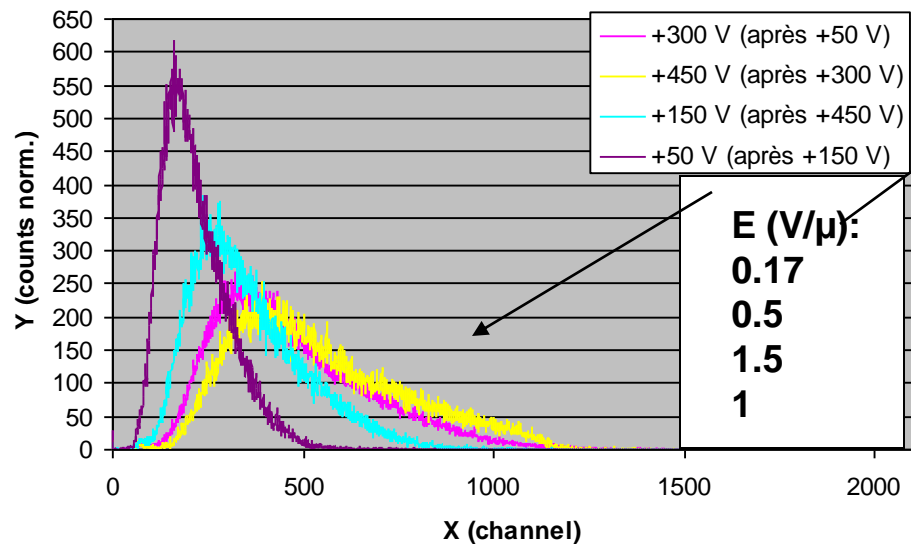
\sim 50 m	GSI ^{124}Xe	GANIL ^{58}Ni	GANIL ^{13}C	GANIL ^{13}C	LPC α
E/A (MeV)	50	10.9	11.1	7.3	1.2
Range (μ)	440	63	196	98	15



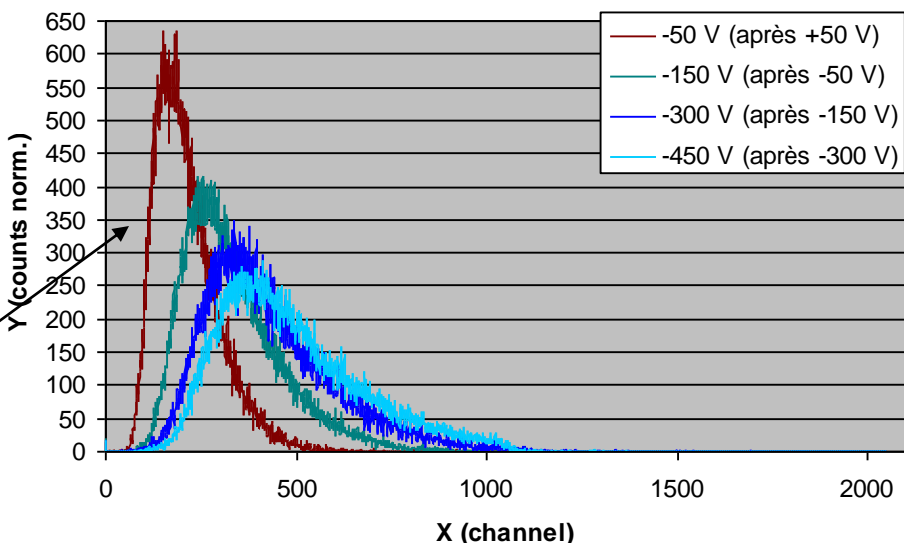
**6.2 GeV ^{124}Xe
(3.4 GeV in 300 μ)**

**GSI: $\sim 3 \times 10^7 \text{ p/spill}$;
 $\sim 3 \times 10^6 \text{ p/det}$ runs of a
few min, for hours**

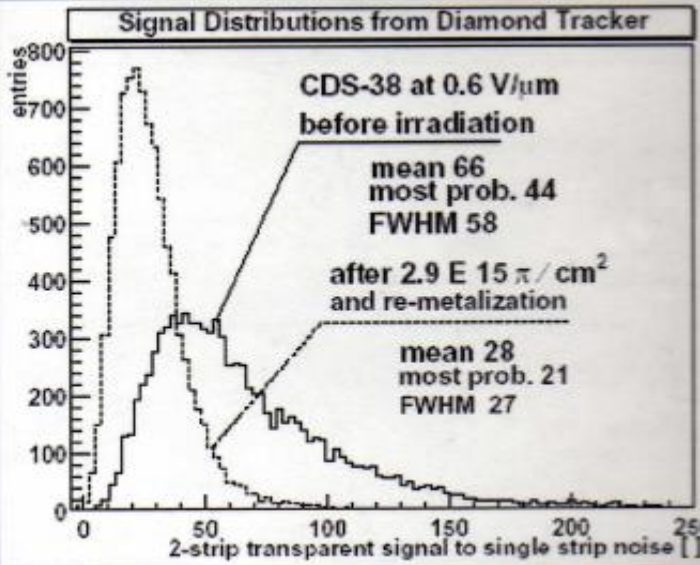
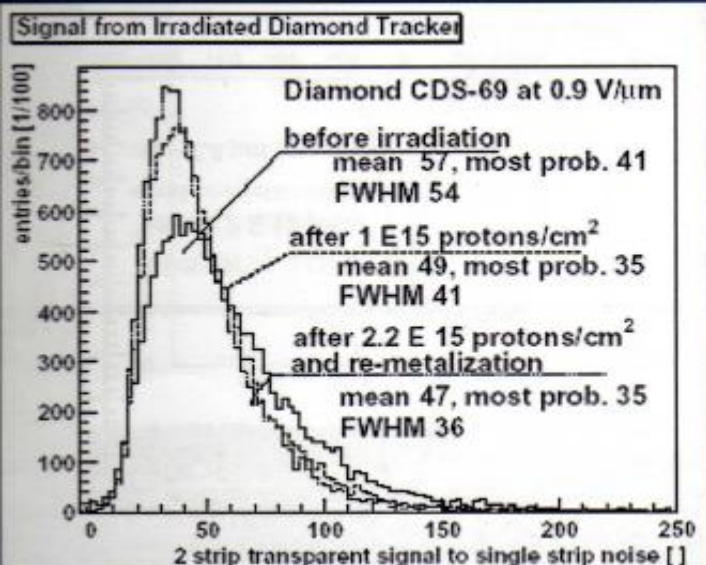
ADC 300 mu; $V > 0$



ADC 300 mu; $V < 0$



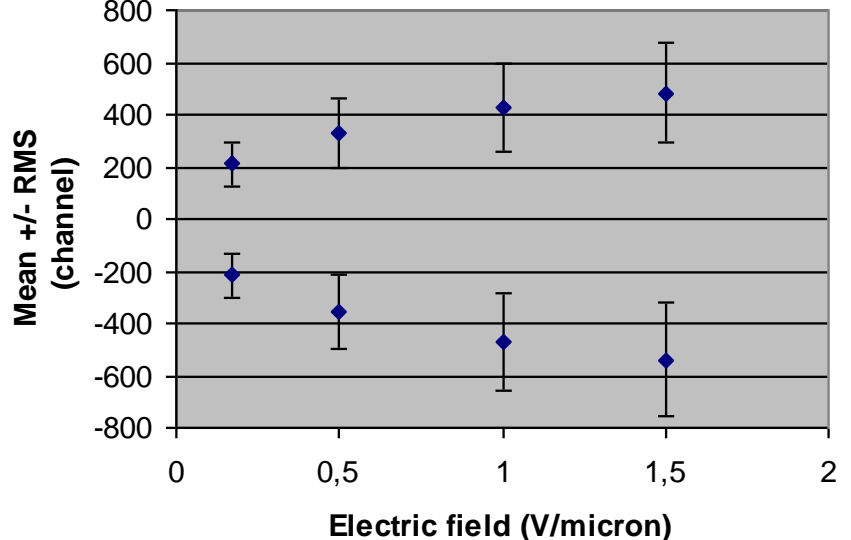
Amplitude spectra: the distribution becomes narrower when the electric field diminishes.



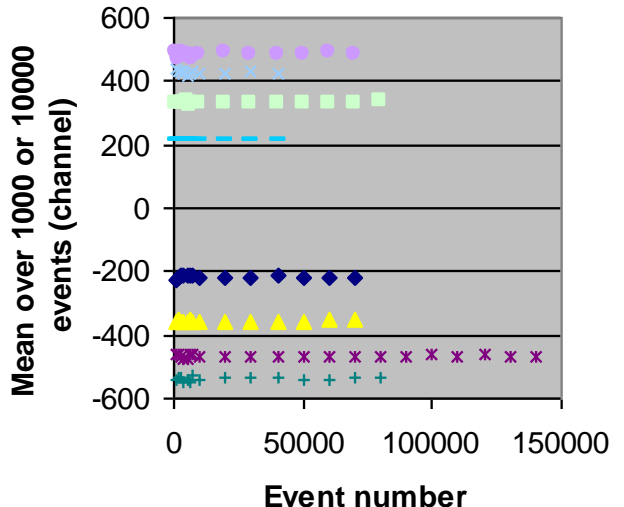
P. Delpierre, RD 42
Journées de prospective du CPPM, 2006

Conjecture: during the irradiation, the electric field may diminish due to the progressive bulk polarization.

6.2 GeV 124Xe (3.4 deposited)

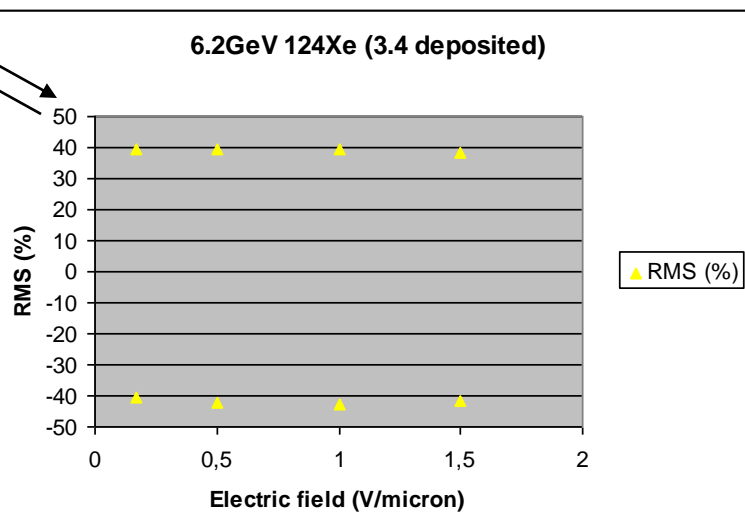


6.2 GeV 124Xe (3.4 GeV deposited)



Slightly better collection (~10%) for $U > 0$, i.e. when the holes coming from the higher carrier density have a shorter drift road.

The relative RMS (%) remains practically the same



Groups of 1000 or 10000 events, chronologically taped, show the same distribution
 ==> no signal attenuation observed

Ramo-Shockley theorem: $i(t) = -q(t) \cdot \vec{v}(t) \cdot \vec{E}^*/1V$

$$q_e = -e; q_h = e$$

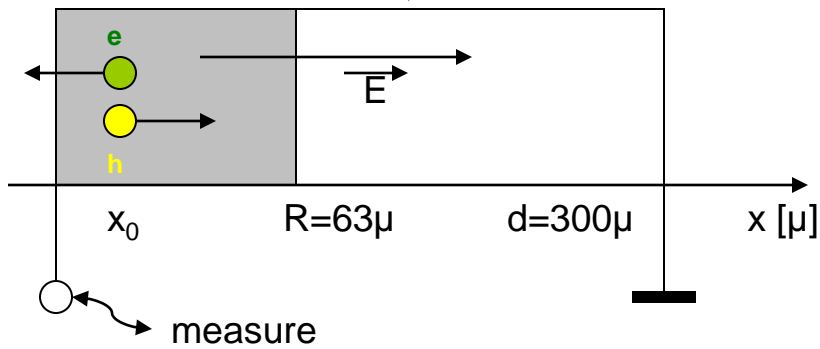
$$v_e = \mu_e * E; v_h = \mu_h * E$$

1V

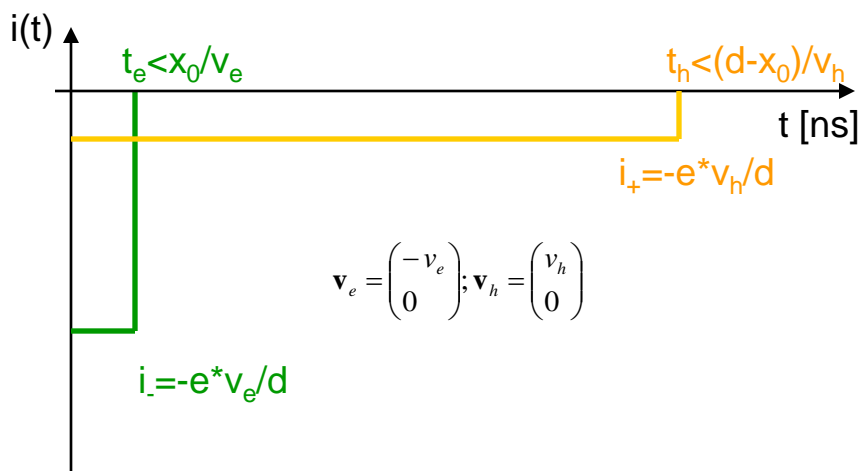
$$\vec{v}_e = \begin{pmatrix} \pm v_e \\ 0 \end{pmatrix}; \vec{v}_h = \begin{pmatrix} \pm v_h \\ 0 \end{pmatrix}$$

$$E^* = \begin{pmatrix} 1V/d \\ 0 \end{pmatrix}$$

0V

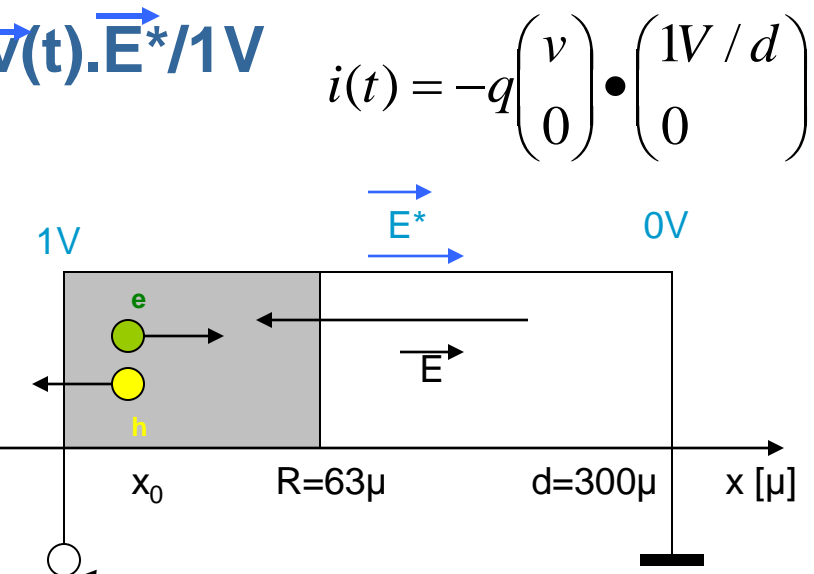


+750V

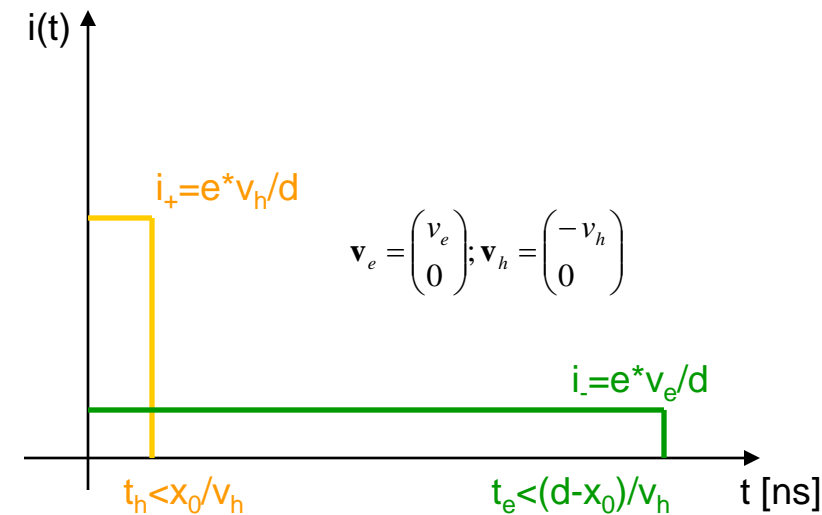


$$\vec{v}_e = \begin{pmatrix} -v_e \\ 0 \end{pmatrix}; \vec{v}_h = \begin{pmatrix} v_h \\ 0 \end{pmatrix}$$

$$i_- = -e^* v_e / d$$



-750V



$$\vec{v}_e = \begin{pmatrix} v_e \\ 0 \end{pmatrix}; \vec{v}_h = \begin{pmatrix} -v_h \\ 0 \end{pmatrix}$$

$$i_- = e^* v_e / d$$

$$t_h < x_0/v_h$$

$$E = 750V/300\mu = 2,5V/\mu; v_h = v_e = v_{sat} = 120\mu/ns$$

$$^{58}\text{Ni}; E=634\text{MeV}; R=63\mu; Q_G=7,813 \text{ pC}$$

^{58}Ni ; E=634MeV; R=63μ;

$$Q_G = 634 \cdot 10^6 \text{ eV} / 13 \text{ eV} \cdot 1,602 \cdot 10^{-19} \text{ C} = 7,813 \text{ pC}$$

$$Q_{e_i} = -0,807 \text{ pC};$$

$$Q_{h_i} = -6,979 \text{ pC};$$

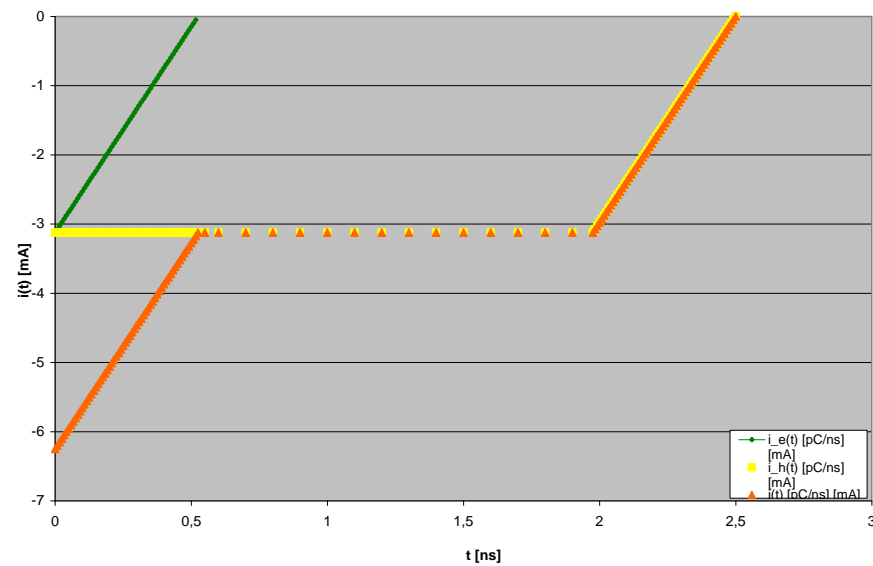
$$Q_i = 7,787 \text{ pC}$$

$$Q_{e_i} = 6,979 \text{ pC};$$

$$Q_{h_i} = 0,807 \text{ pC};$$

$$Q_i = 7,787 \text{ pC}$$

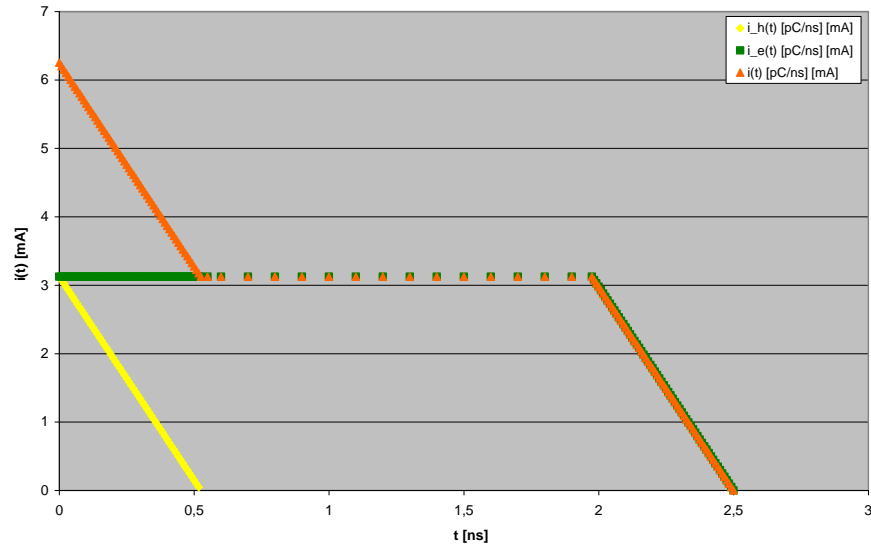
Current pulse calculated on the Growth side, irradiated - det1: Gs +750 V



$$E = 750 \text{ V} / 300 \mu\text{s} = 2,5 \text{ V}/\mu\text{s}; v_h = v_e = v_{sat} = 120 \mu/\text{ns}$$

electrons: short drift way

Current pulse calculated on the Growth side, irradiated - det1: Gs -750 V



electrons: long drift way

$$-\frac{dq}{dx} = q/w_s$$

$$q(x) = q_0 \exp(-x/w_s)$$

$$q(t) = q_0 \exp(-t/t_s)$$

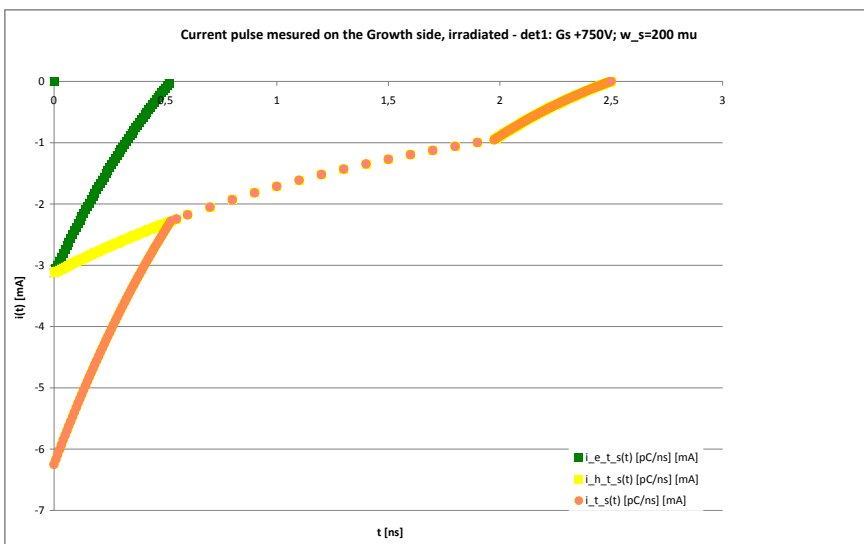
$w_s \approx 200 \mu$ (E. Griesmayer et al., "High-Resolution

Energy and Intensity Measurements with CVD Diamond at REX-ISOLDE",

CERN BE-Note-2009-028) $t_s = w_s / v_{sat} = 1,67 \text{ ns}$

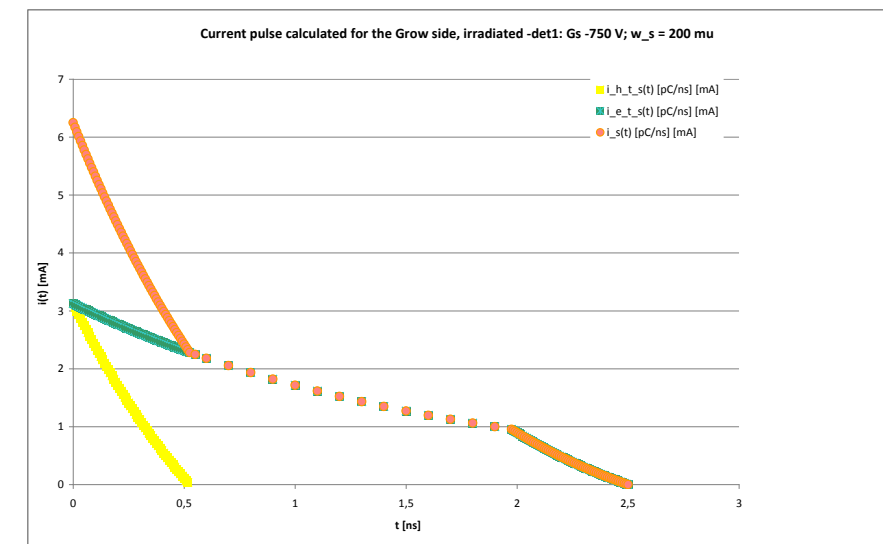
$$Q_{e_C} = Q_G \frac{w_s}{R} \left(1 - e^{-\frac{R}{ws}} \right) = -6,072 \text{ pC};$$

$$Q_{h_C} = Q_G \frac{w_s}{R} \left(e^{-\frac{d-R}{ws}} - e^{-\frac{d}{ws}} \right) = -2,049 \text{ pC};$$



$$Q_{h_C} = Q_G \frac{w_s}{R} \left(1 - e^{-\frac{R}{ws}} \right) = +6,072 \text{ pC};$$

$$Q_{e_C} = Q_G \frac{w_s}{R} \left(e^{-\frac{d-R}{ws}} - e^{-\frac{d}{ws}} \right) = +2,049 \text{ pC};$$

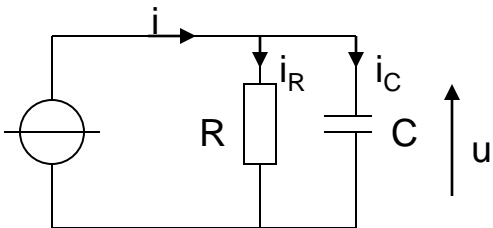


$Q_{e_i} = -0,728 \text{ pC};$
 $Q_{h_i} = -3,773 \text{ pC};$
 $Q_i = -4,500 \text{ pC}$

electrons:
short drift way

$Q_{e_i} = +0,728 \text{ pC};$
 $Q_{h_i} = +3,773 \text{ pC};$
 $Q_i = +4,500 \text{ pC}$

electrons:
long drift way



$C = 89 \text{ pF}$;
 $R = 50 \Omega$;
 $\tau = RC = 4,45 \text{ ns}$

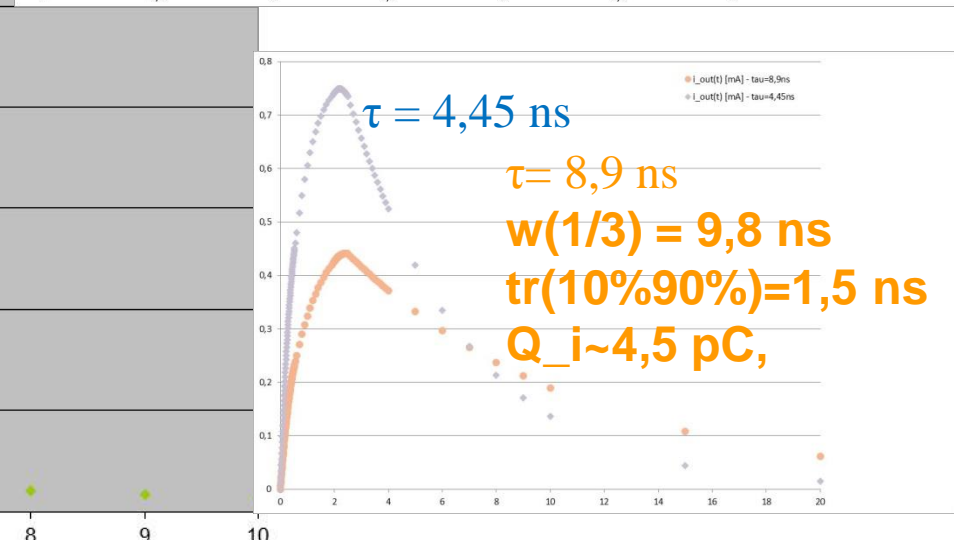
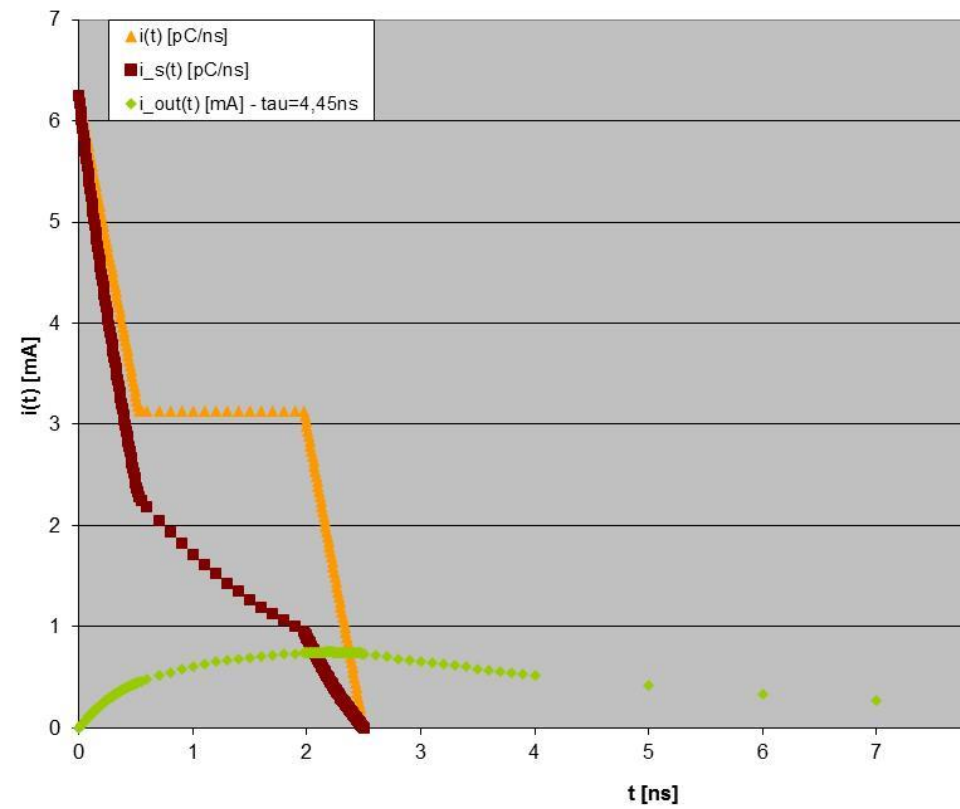
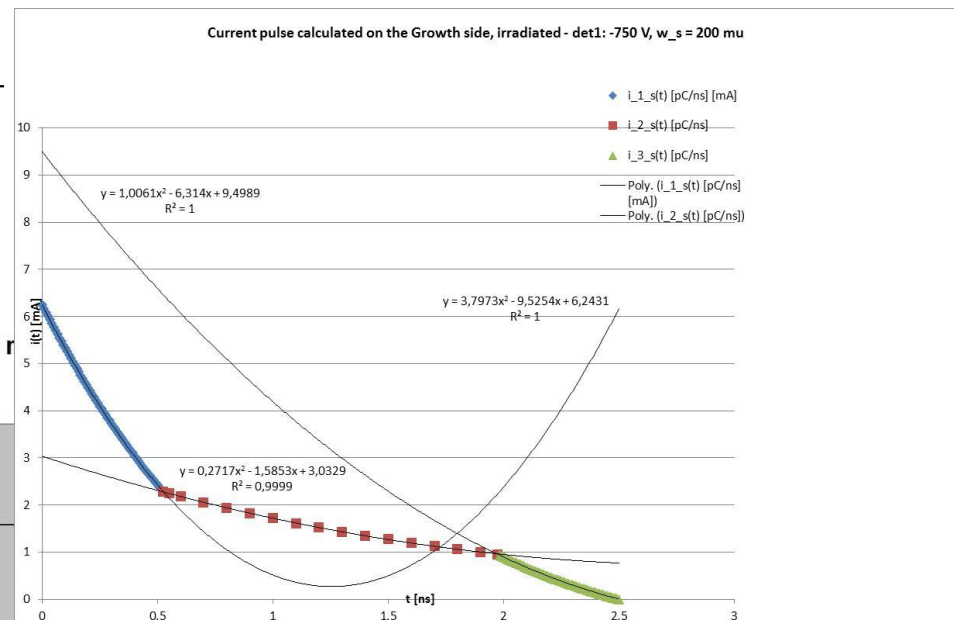
$$i(t) = \frac{u(t)}{R} + C \frac{du(t)}{dt}$$

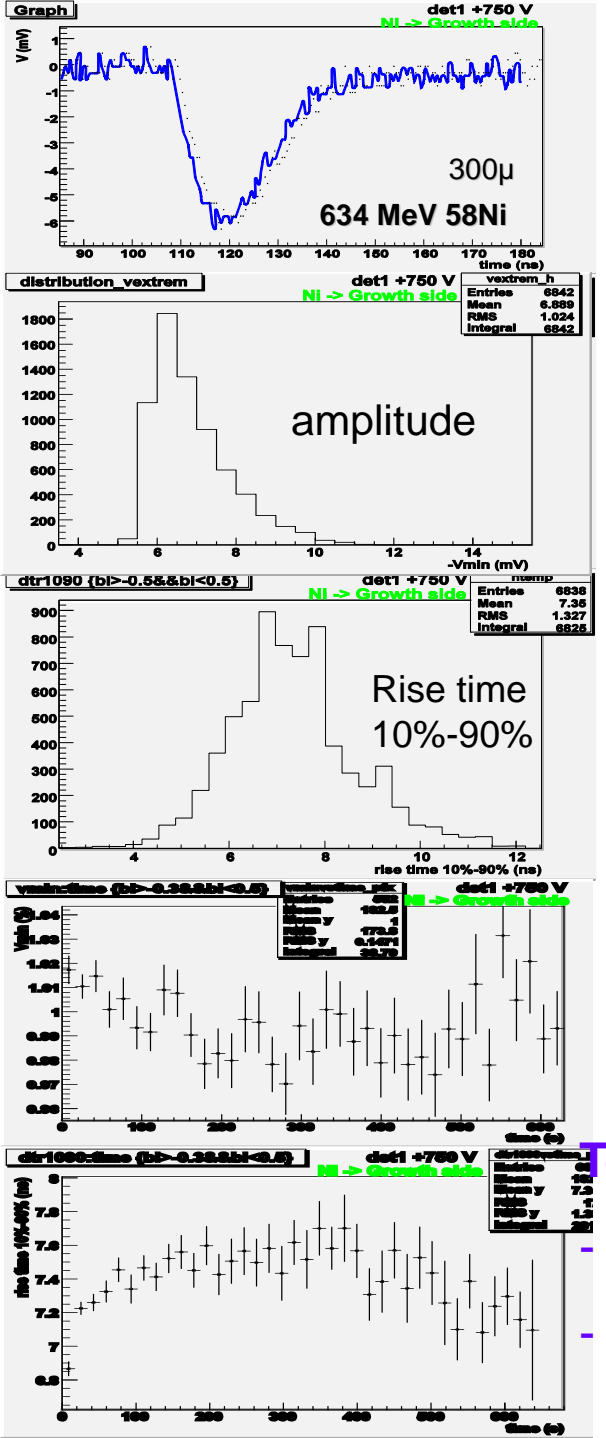
$$i(t) = I_{0j} + a_j t + b_j t^2; j=1,2,3$$

$$u(t) = D_i * \exp(-t/\tau) + V_{0i} + A_i t + B_i t^2$$

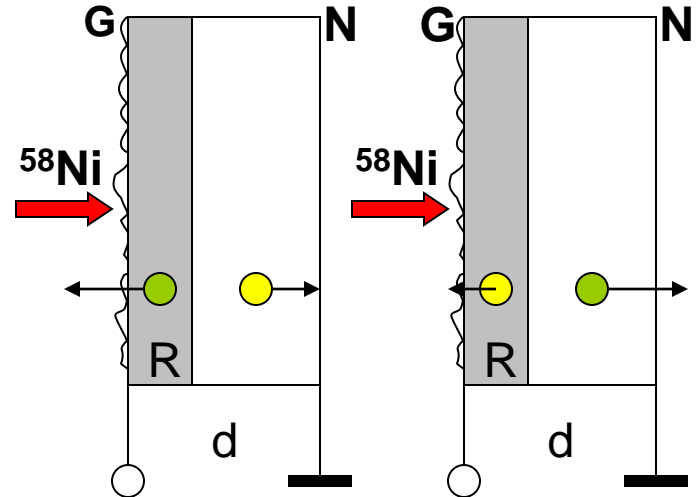
$w(1/3) = 7,8 \text{ ns}$
 $tr(10\%90\%) = 1,4 \text{ ns}$
 $Q_i \sim 4,5 \text{ pC}$

MATACQ – VME (400 MHz BW) 0,9ns 70 m cable





d - thickness; R – range: R<<d



+750V

$0 \leq S_e \leq R$

$d-R \leq S_h \leq d$

-750V

$0 \leq S_h \leq R$

$d-R \leq S_e \leq d$
favourable

S_e – drift électrons –



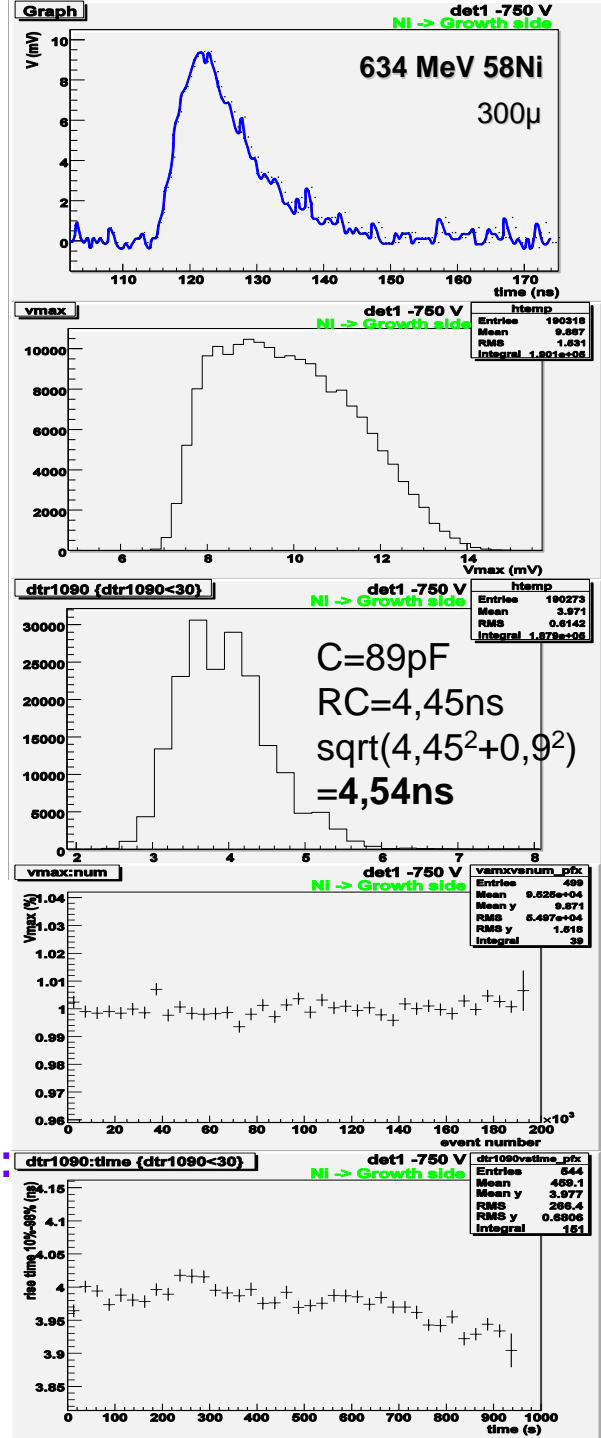
S_h – drift holes +

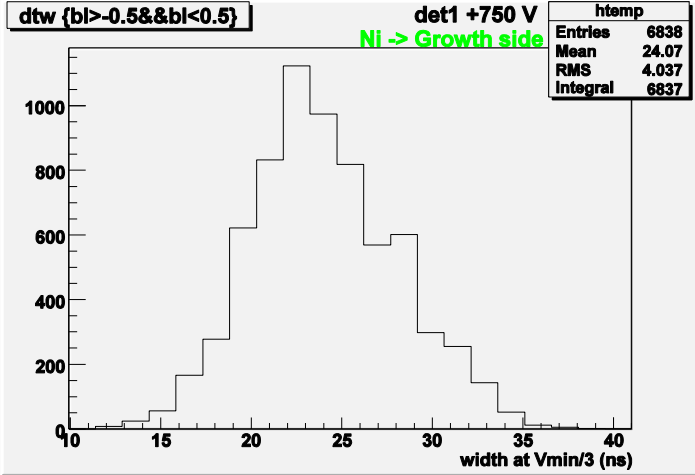


Tests - not-segmented detectors:

- $S_h < S_e$ – favourable
- d adequate to R

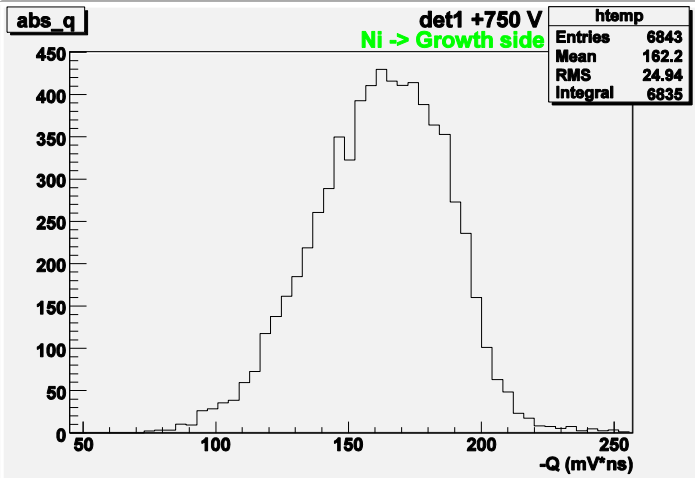
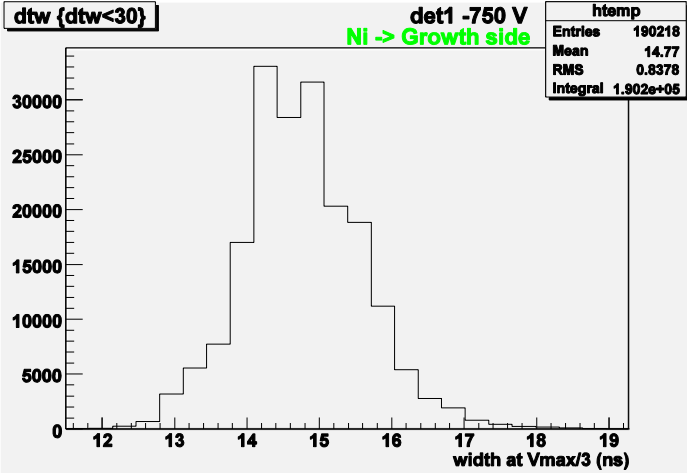
GANIL – SME: $\sim 10^4$ pps



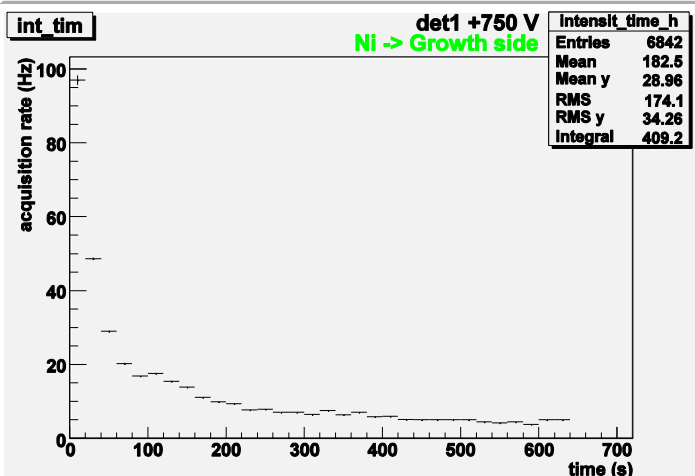
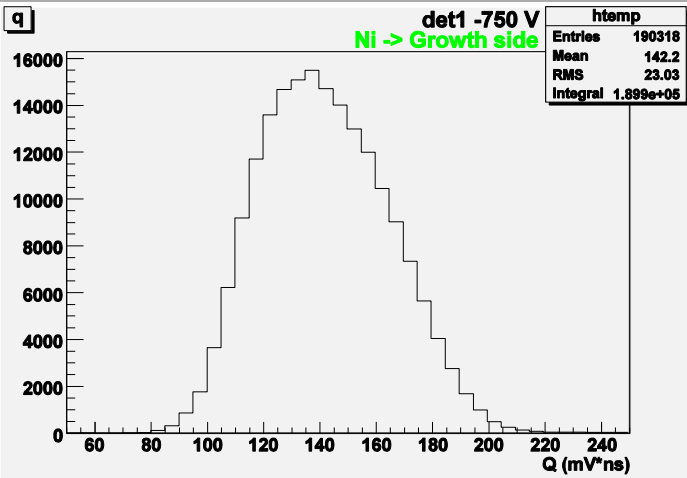


300 μ ; E = 2,5 V/ μ

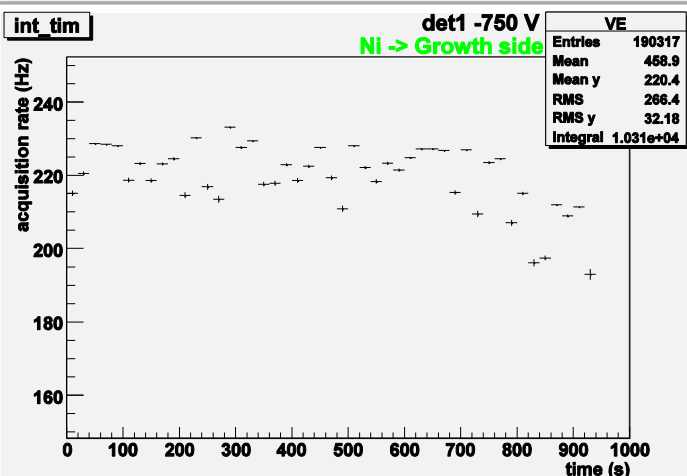
Width at 1/3Vextrem (ns)

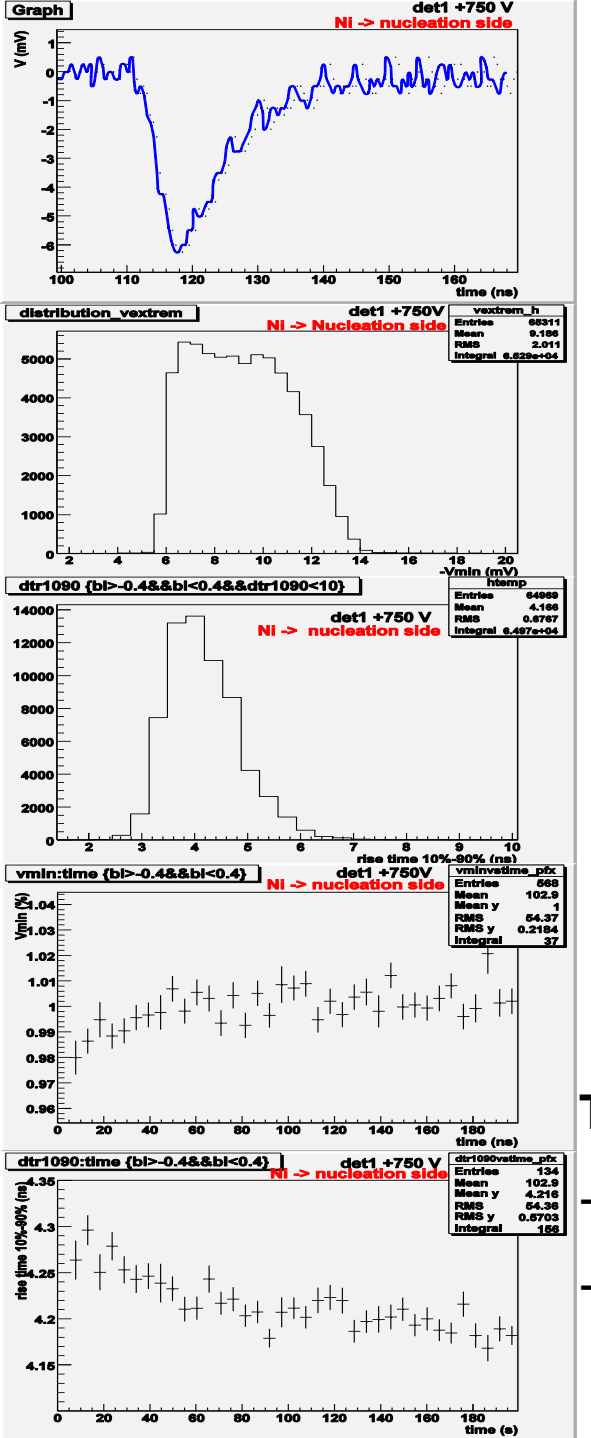


Charge (mV*ns)

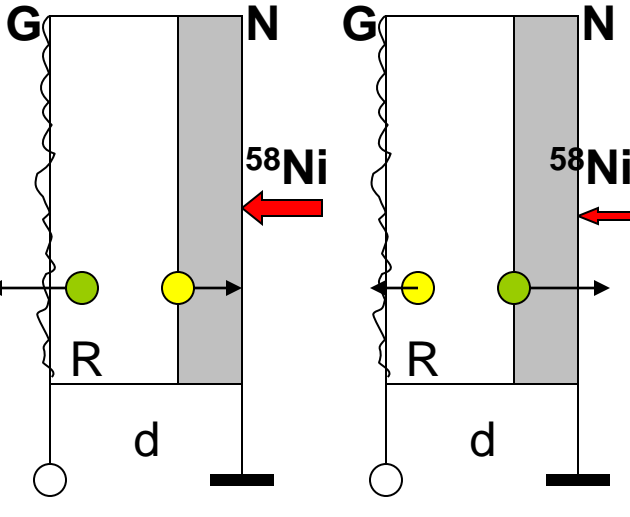


Acquisition rate (Hz)





d - thickness; R – range: R<<d



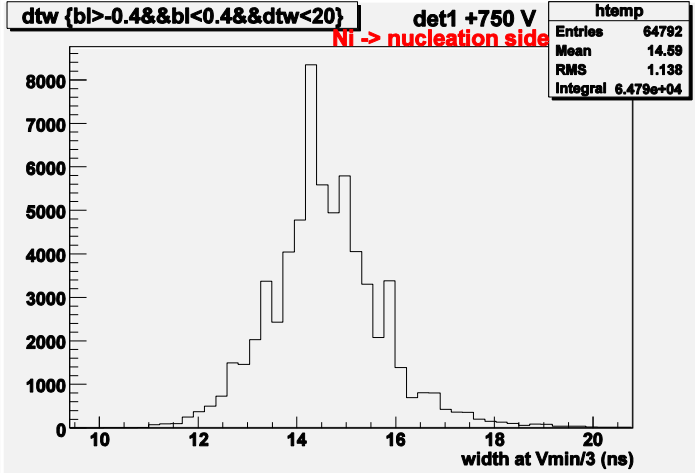
S_e – drift **électrons** -

S_h – drift **holes** +

Tests - not-segmented detectors:

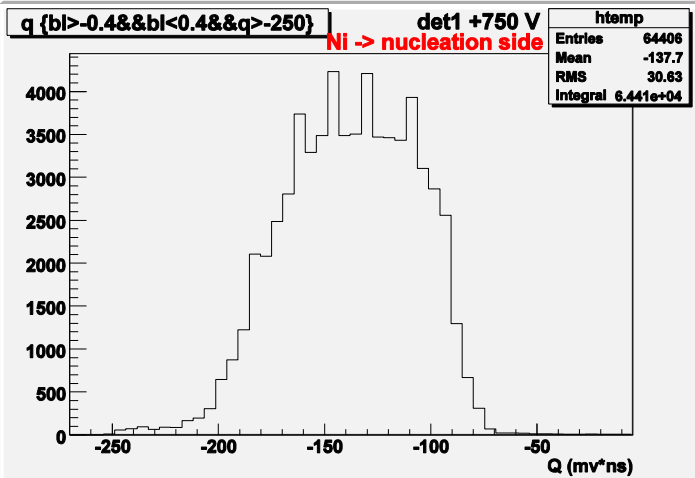
- $S_h < S_e$ – favourable
- d adequate to R

GANIL – SME: $\sim 10^4$ pps

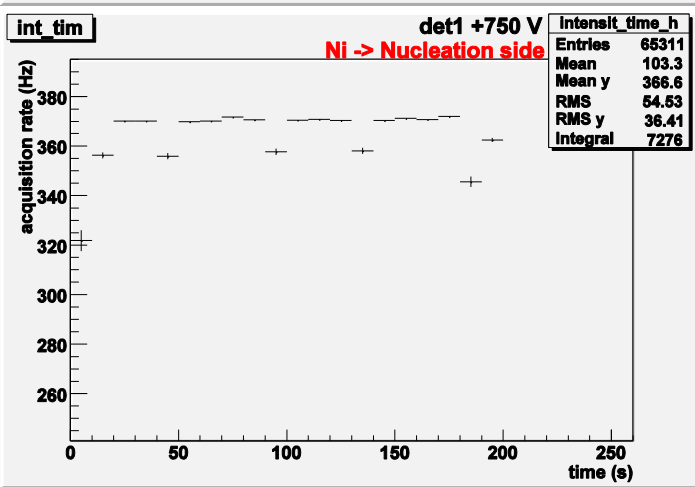
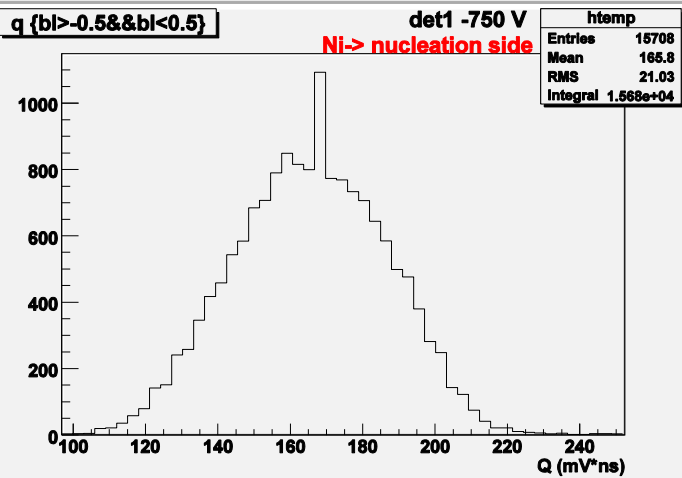
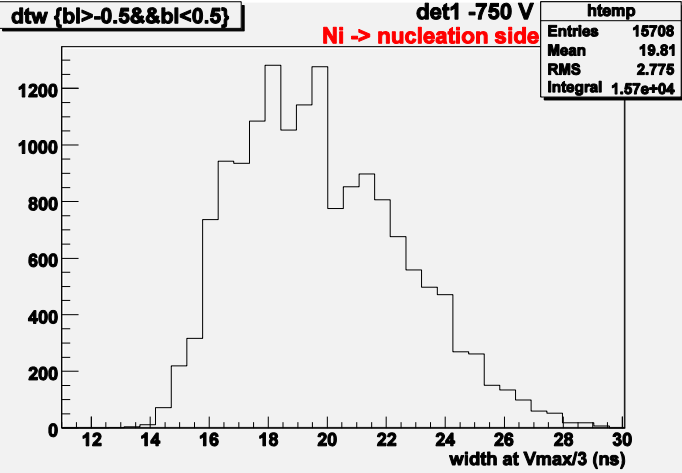


300 μ ; E = 2,5 V/ μ

Width at 1/3Vextrem (ns)



Charge (mV*ns)



Acquisition rate (Hz)

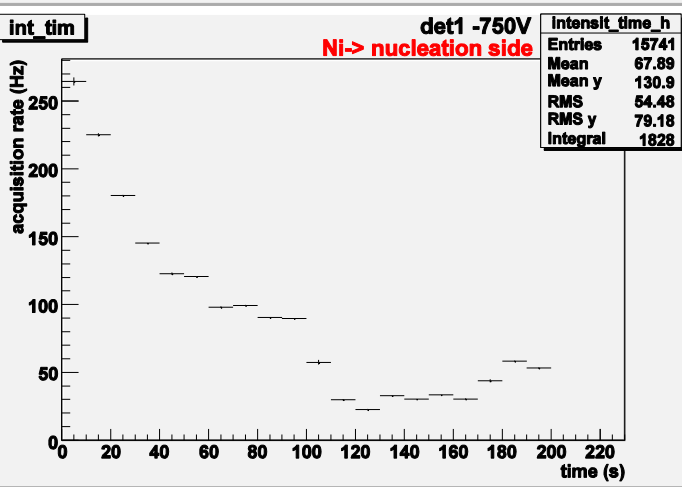
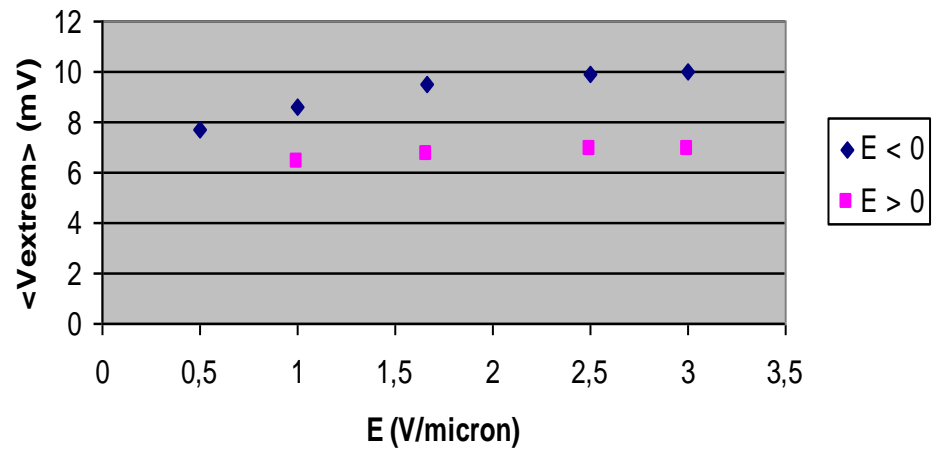


Table 3. Synthetic results concerning the shape of the signal induced by 634 MeV ^{58}Ni ions, having a range of ~ 60 μm in a uni-strip diamond detector **P1N ELA** of 300 μm at $E = 2,5 \text{ V}/\mu\text{m}$.

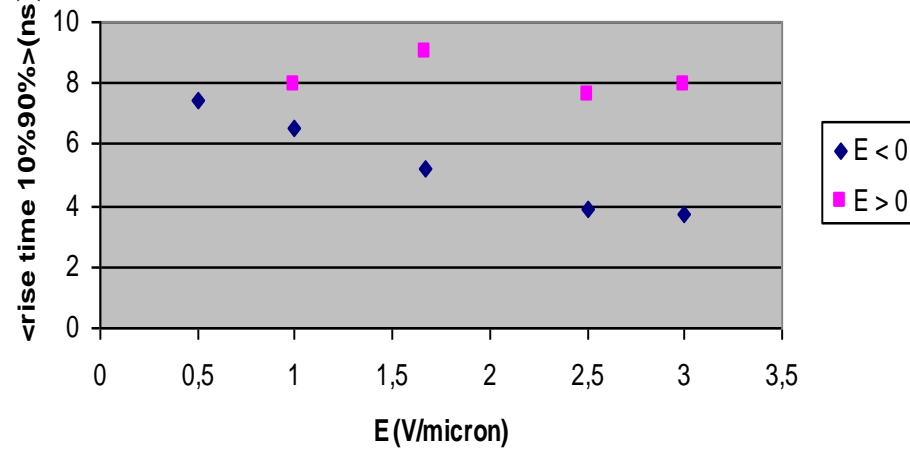
irradiated face	G face U (V) long tranzit	$\langle V_{\text{extrem}} \rangle$ (mV)	Rms V (mV)	$\langle Q \rangle$ (mV*ns)	Rms Q (mV*ns)	tr (ns)	rms tr (ns)	$\langle w_{1/3} \rangle$ (ns)	Rms w (ns)
G	+750 holes	6.9	1.0	162	25	7.4	1.3	24.1	4.0
G	-750 electrons	9.9	1.5	142	23	4.0	0.61	14.8	0.84
N	+750 electrons	9.2	2.0	138	31	4.2	0.68	14.6	1.1
N	-750 holes	8.8	1.2	166	21	6.1	1.1	19.8	2.8

Faster and higher signals are generally preferred for beam monitoring. The conclusion emerging from Table 2 is that, when the range of the ion is much shorter than the detector thickness and the distances of drift for the two types of carriers to the electrodes are different, the voltage has to be chosen in such a way that the holes have the shortest drift road, regardless of the irradiated side. This will have several beneficial effects: higher signal amplitude, shorter signals, characterized by a faster rise time and a shorter fall too. The quality of the signals, somehow better on the fourth line of the table as compared to that on the first line - both of them concerning the long drift distance for the holes – may show that the signal degradation is a little bit smaller when their road leads to the growth side, with bigger diamond crystallites and therefore a higher quality (for the fourth line) than when their road leads towards the nucleation side, including more graphite (first line).

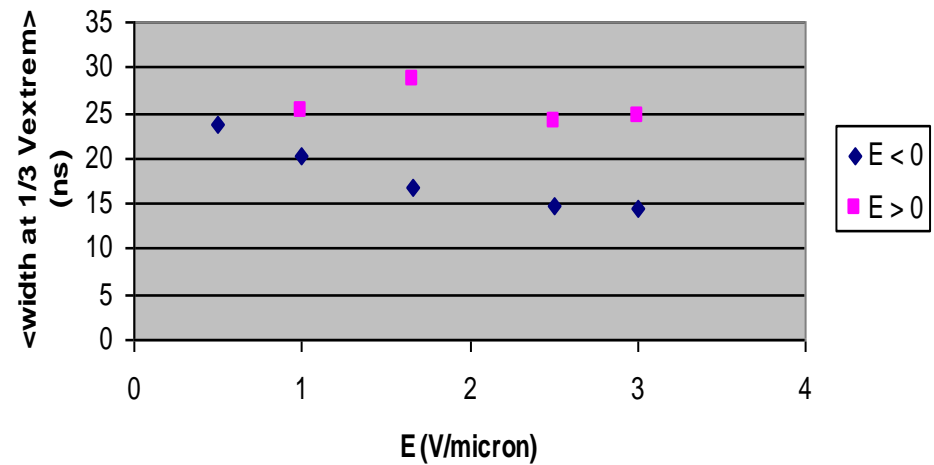
det1; Ni -> Growth side



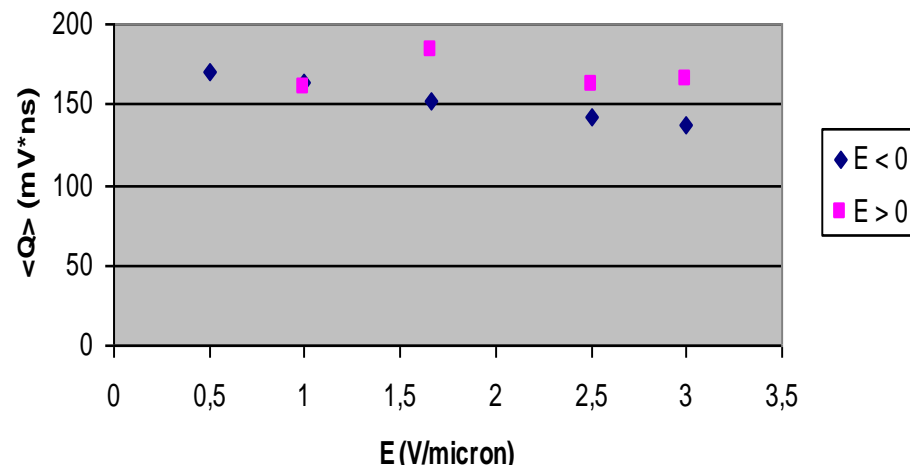
det1; Ni -> Growth side



det1; Ni -> Growth side



det1; Ni -> Growth side



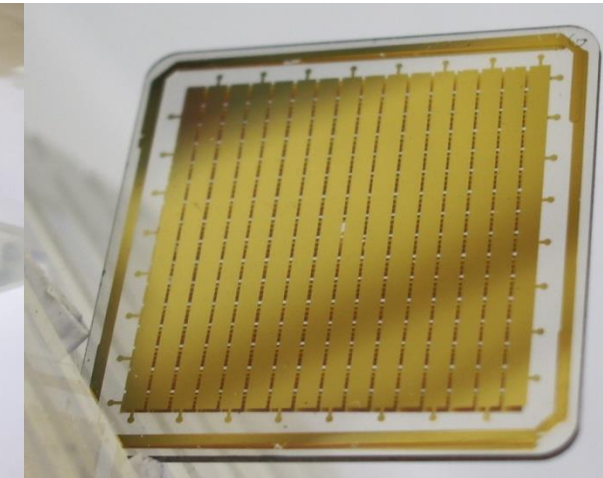
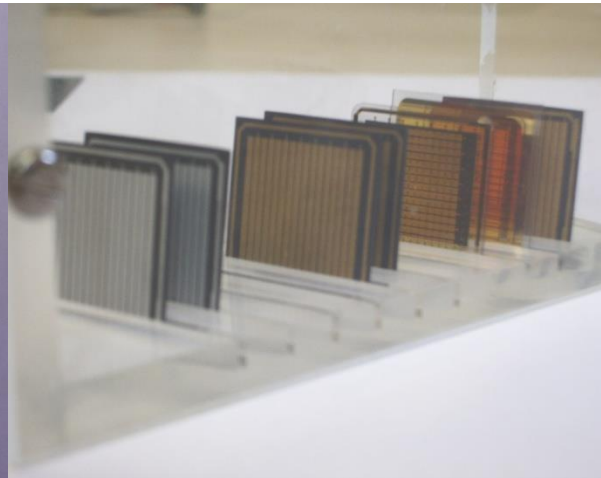
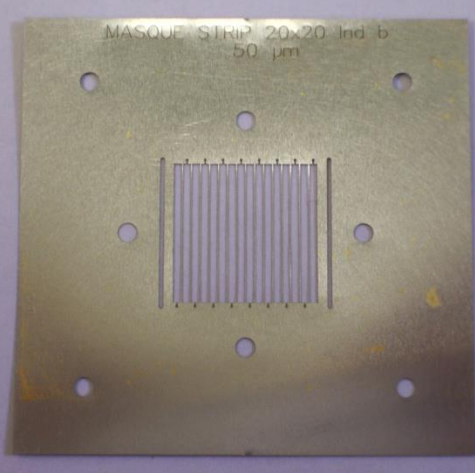
When $R < d$, the signal is higher and faster when the **electrons** drift on a **longer** way then the **holes**.

Similar results for det2

IV Multi-strip detectors: Company 1 - ELP vs ELS

ELP (Electronic Premium Grade) – processed from a polycrystalline wafer with a starting thickness of 1 mm; the final thickness is achieved by removal from the nucleation surface; therefore, thinner the thickness of an ELP plate is, higher its quality; but under 0.2 mm, the risk of breaking in the process of lapping and polishing is much increasing;

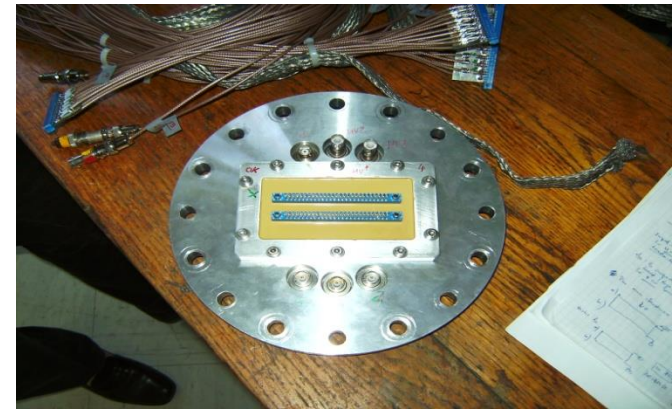
ELS (Electronic Standard Grade) – processed from a polycrystalline wafer with a minimum removal of 100 µm. Comparing the two types of material was one of the objectives of our study.



Strip pitch: 0.9mm
inter-strip gap: 0.1mm
efficiency: 90%

The BERGER files for
the masks & PCBs
were done at LPC

Flange and
connectors



Det III:

5.5 MeV α

PRL:
developped
at LPC

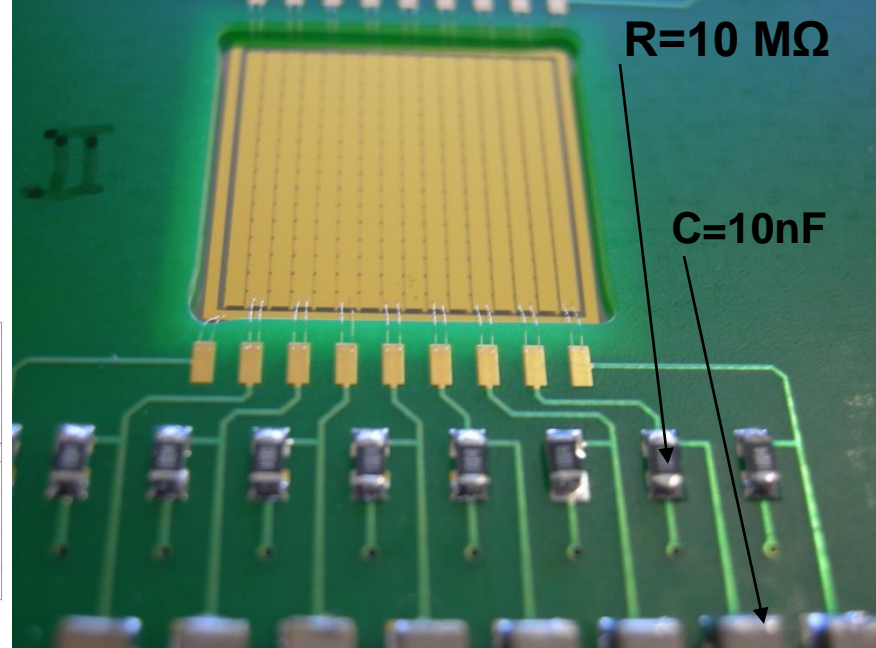
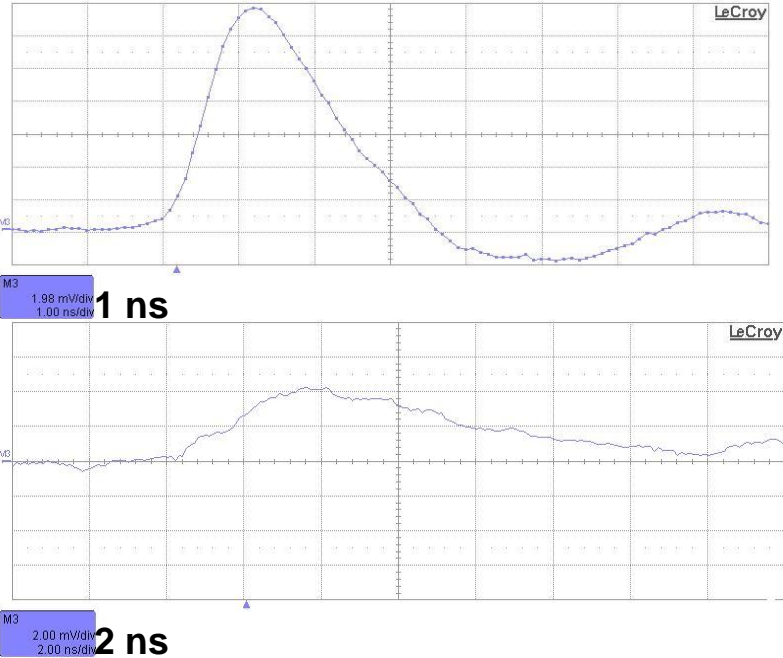
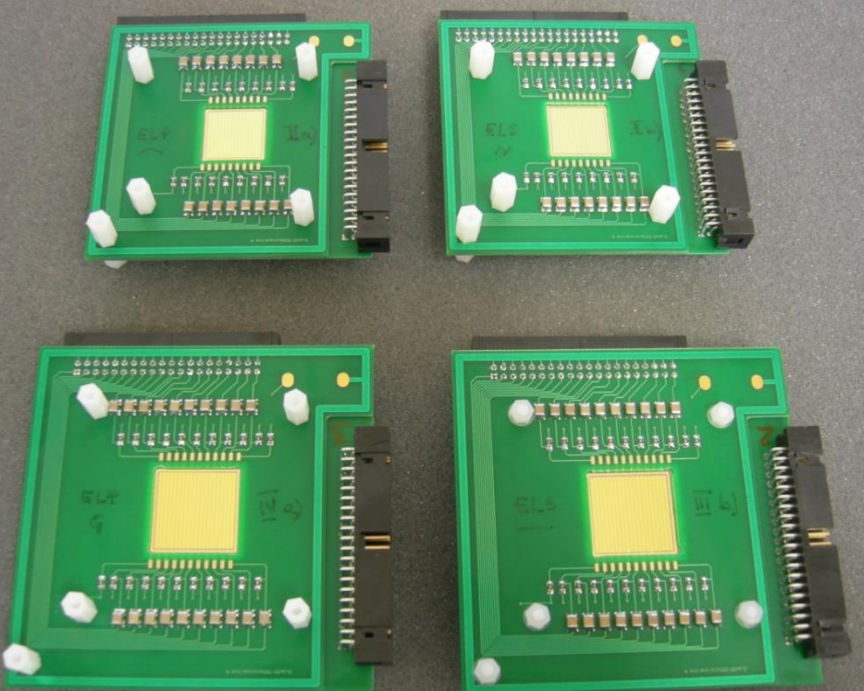
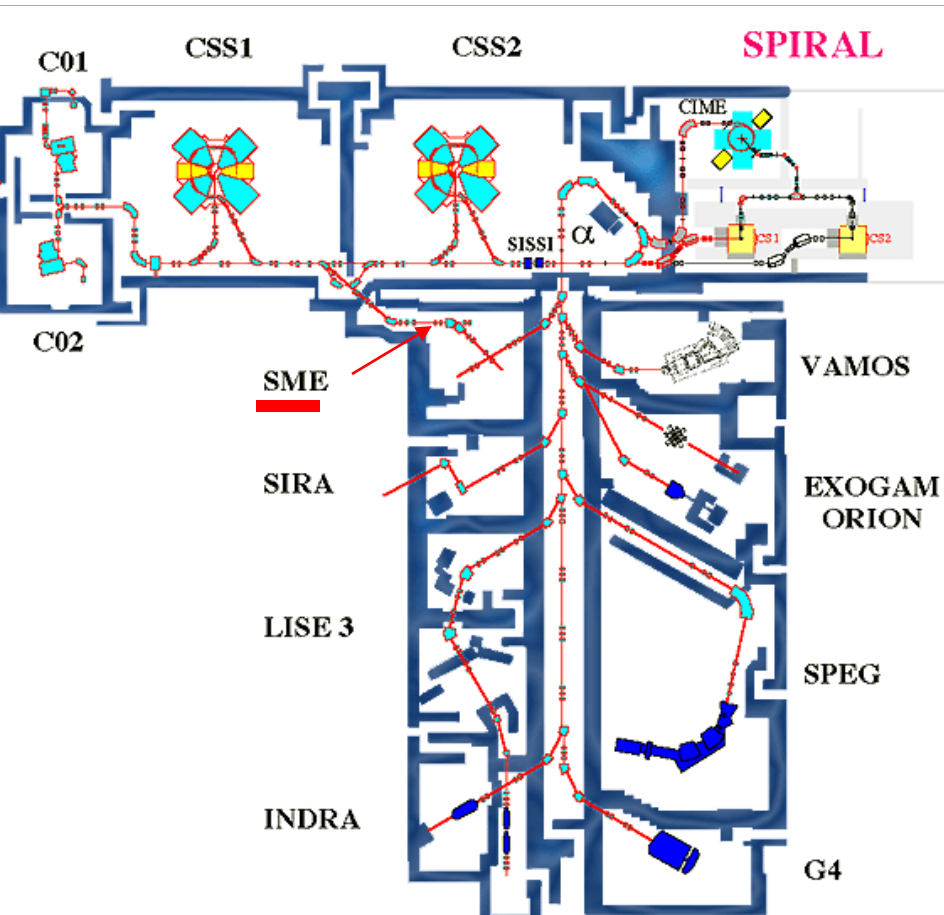


Table 3. the multi-strip detectors built at LCP; a) and b) are the 2 faces

Detecteur	P2 - Type	Densité (g/cm ³)	Epaisseur (μm)	Surface active (mm ²)	Nombre de pistes
I	ELS	2.9	565	16x16	a) 16 G b) 16 N
II	ELP	3.4	575	16x16	a) 16 b) 16
III	ELS	2.9	240	20x20	a) 1 b) 20
IV	ELP	3.4	350	20x20	a) 20 b) 20



Les tests au GANIL: sur la ligne SME (sortie moyenne énergie)



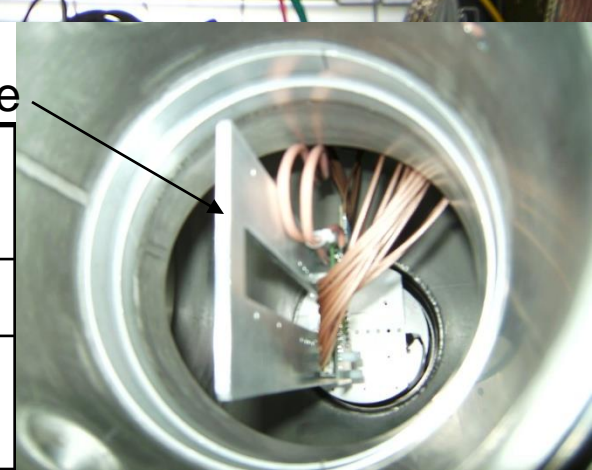
Installation des détecteurs



Table 4. Ions used in GANIL

Plaque + détecteur + alumine

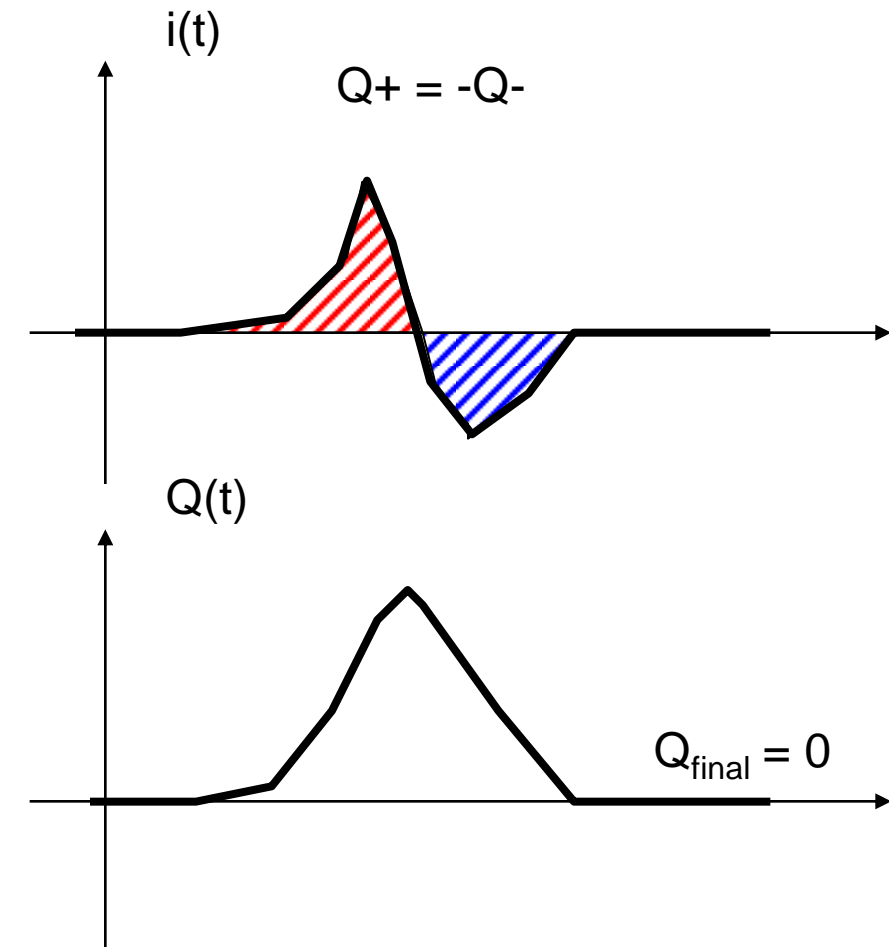
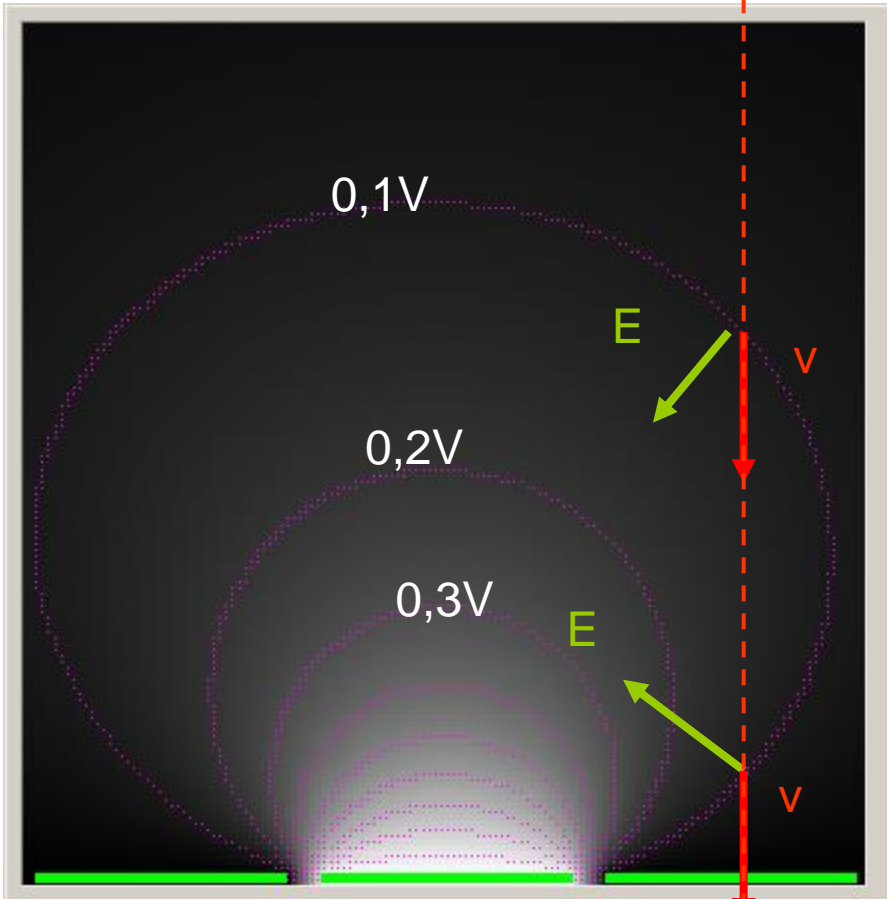
$\sim 2,5$ m	GANIL ^{70}Zn	GANIL ^{36}S	GANIL ^{36}S	GANIL ^{16}O	LPC α
E/A (MeV)	8.7	7.2	3.9	13.7	1.2
Range (μ) ELS	63	48	26	225	15
range (μ) ELP	55	42	22	198	13



Cours Jean-Marc Fontbonne



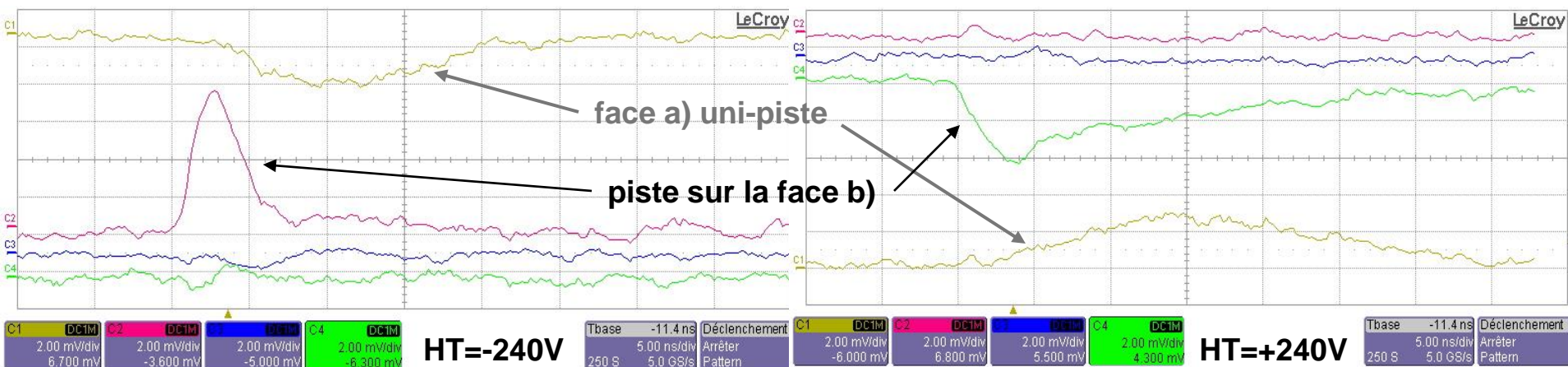
Induction d'un signal transitoire sur les pistes adjacentes



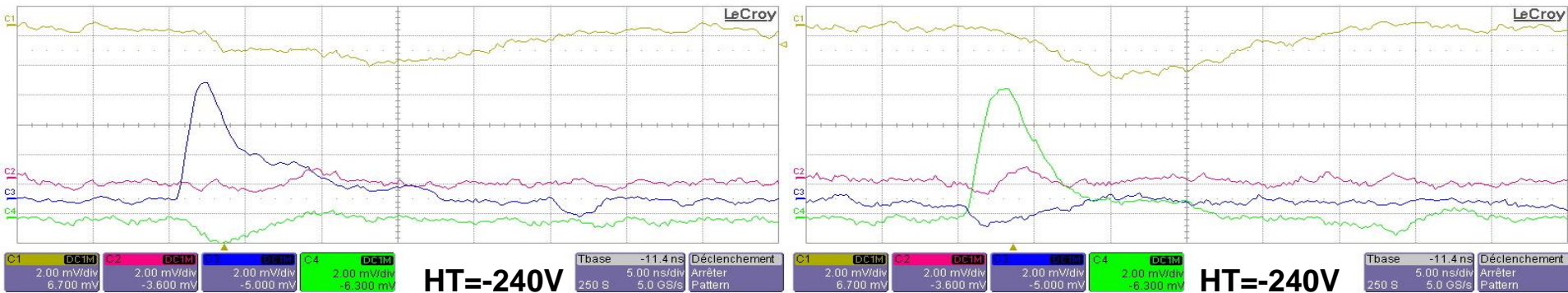
Il peut également y avoir des problèmes sur les interpistes
→ Répartition du signal sur des pistes contigües

Résultats pour les détecteurs multipiste: images prises sur l'oscilloscope LeCroy

HT sur la face b) irradiée ($1V/\mu$)



Signals induced by ^{36}S of 7.2 AMeV in the detector III of ELS type

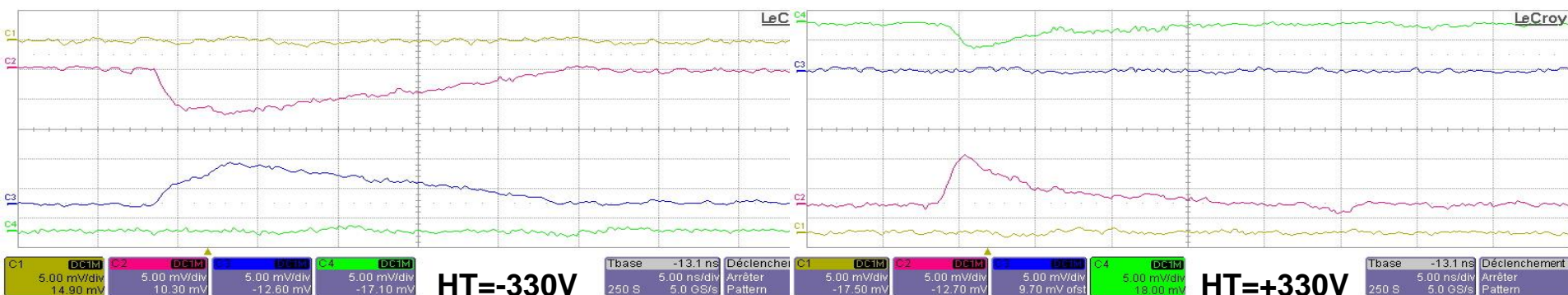


Signals induced by ^{36}S of 7.2 AMeV in the detector III of ELS type: examples of cross-talk between neighbouring strips on the irradiated face (blue and green)

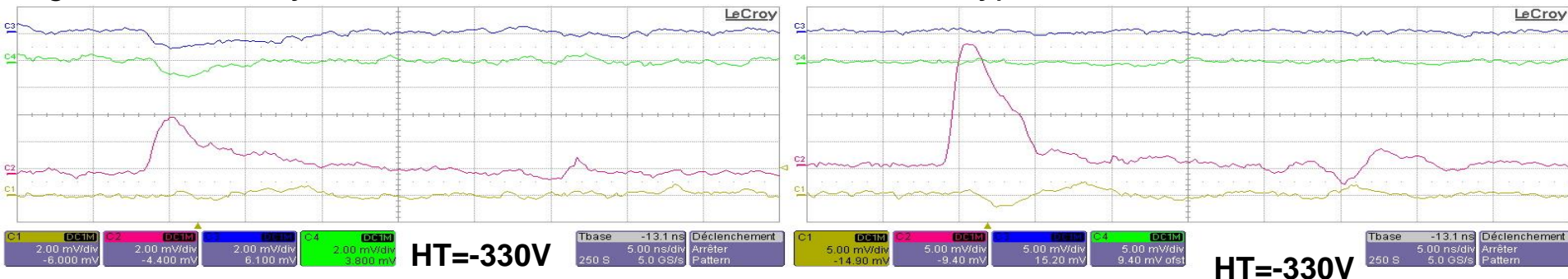
Résultats pour les détecteurs multipiste: images prises sur l'oscilloscope LeCroy

Coincident signals on the two sides of the detector

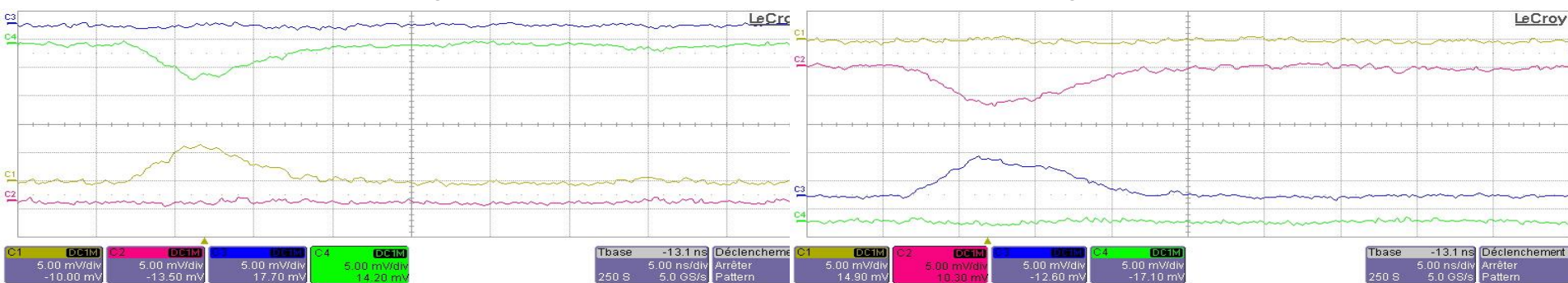
HT sur la face a) irradiée (1V/ μ)



Signals induced by ^{36}S of 7.2 AMeV in the detector IV of ELP type

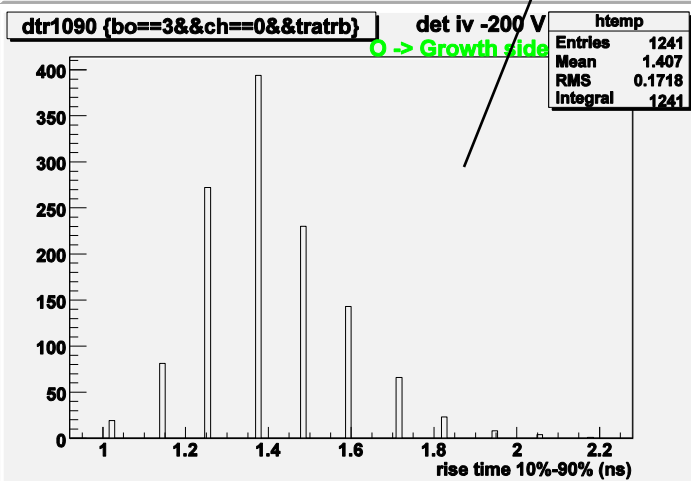
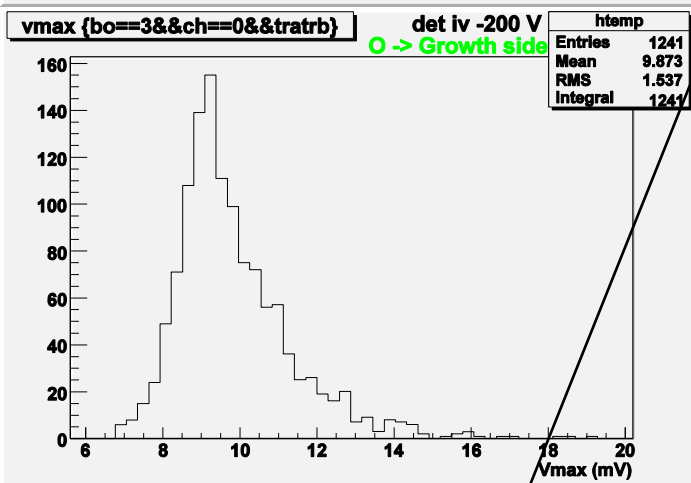
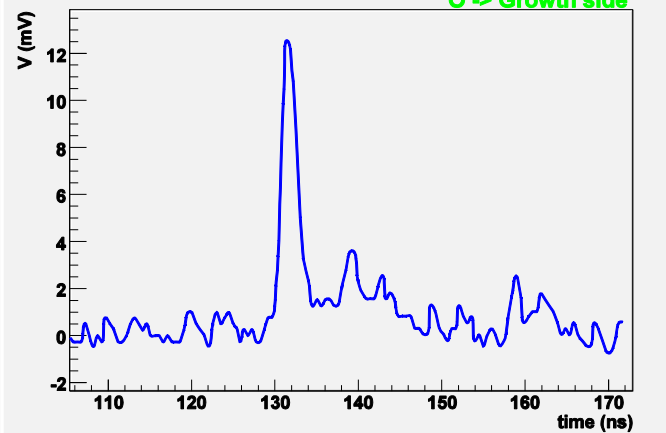


The particle is probably passing between strips (left); example of cross-talk (right)



Signals induced by ^{36}S of 3.9 AMeV in the detector IV of ELP type (-330 V)

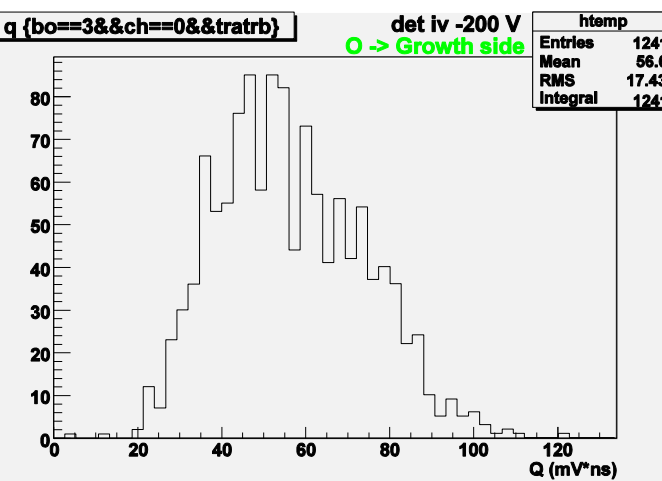
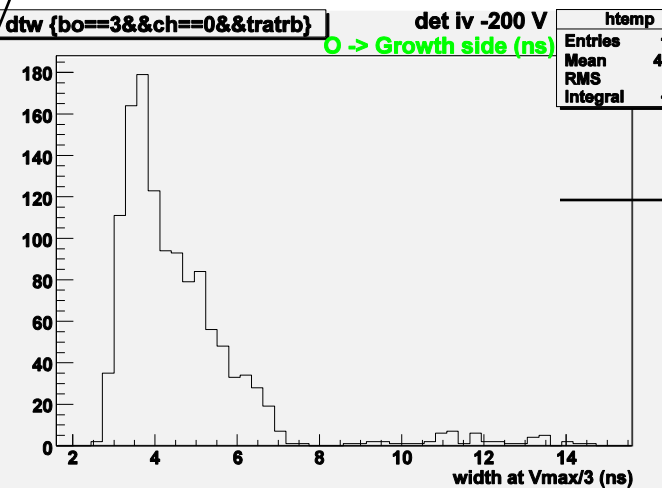
Graph



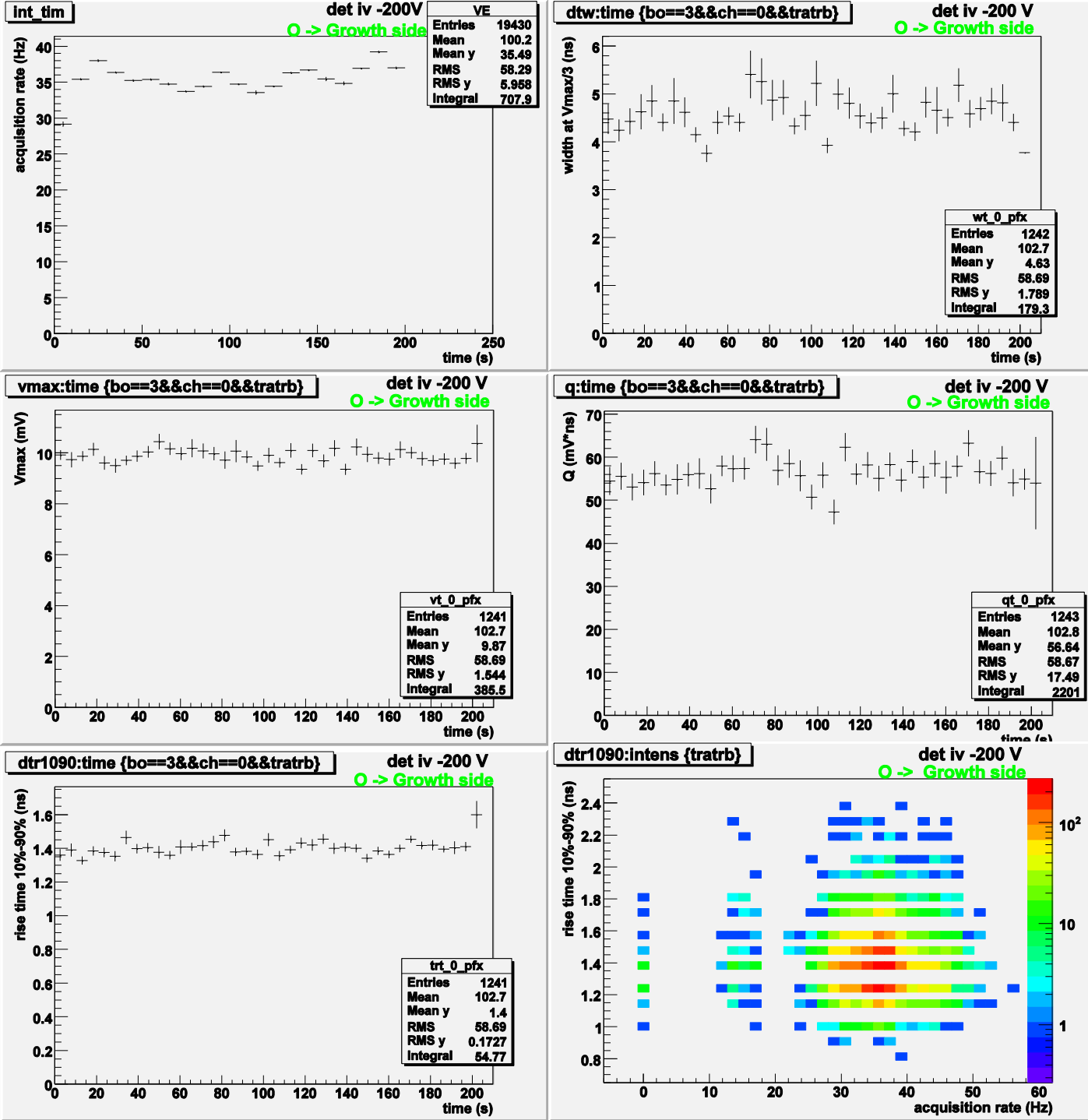
Det iv ELP, 350 μ , -200 V,
E=0.6V/ μ board 3, channel 0;
O → Growth side: 13.7 AMeV

S=18mm²; C=2,57 pF RC=0,13ns

Matacq → 0,9 ns



Acquisition:
MATACQ – VME
(400 MHz BW;
2GHz sampling) –
12 channels
- oscillo LeCroy
64Xi (600 MHz BW;
10Gs/s) –
4 channels



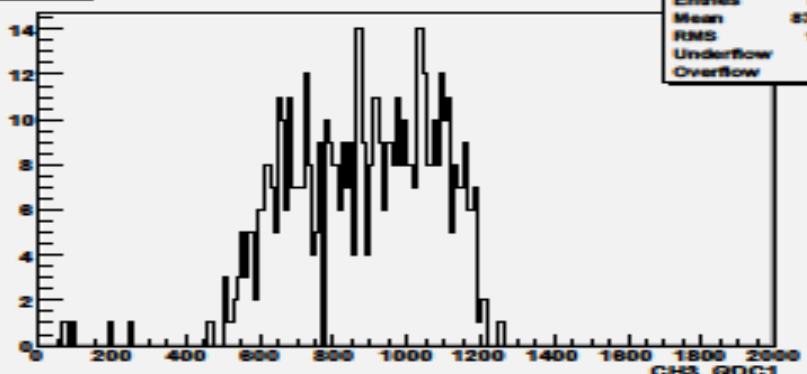
Det iv ELP, 350 μ
-200 V, E=0.6V/ μ
board 3;
O: 13.7 AMeV

Det_8x8_pistes (ELS - 300μm: TiPtAu);

Piste4_4_-750V_nuclear

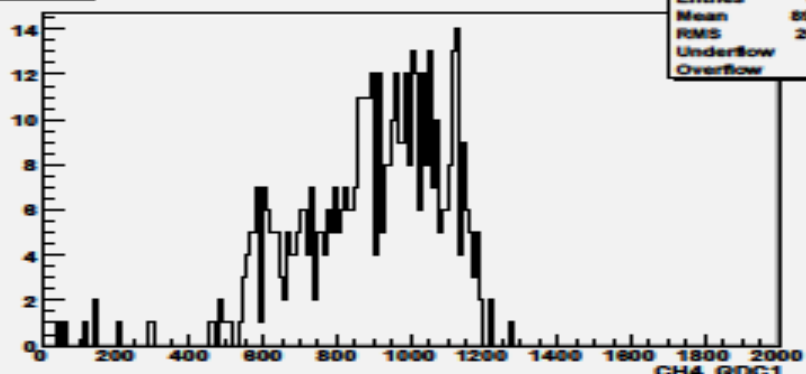
HV = -750 V on Nucleation; source α on Growth, PRL1, FASTER

CH3_Q1



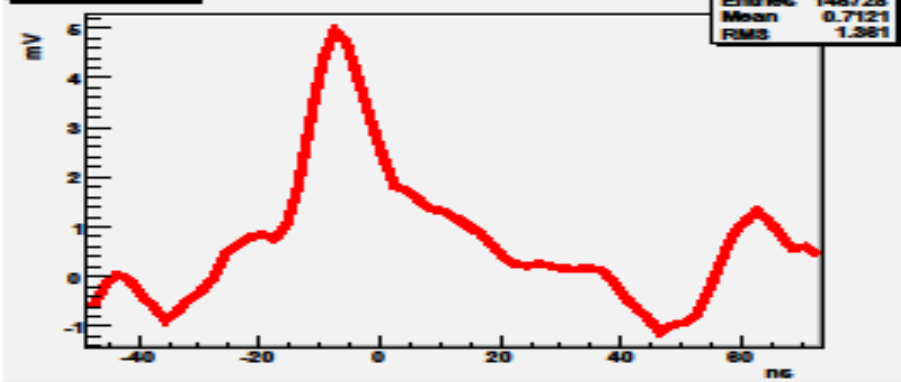
CH3_QDC1

CH4_Q1



CH4_QDC1

CH4_Oscillo



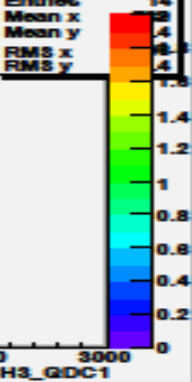
CH4_Oscillo

CH3_QDC1

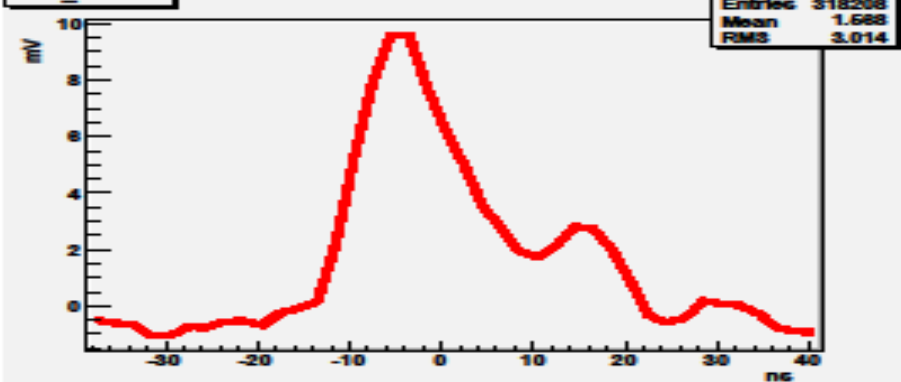


Laboratoire de physique corpusculaire

correlation



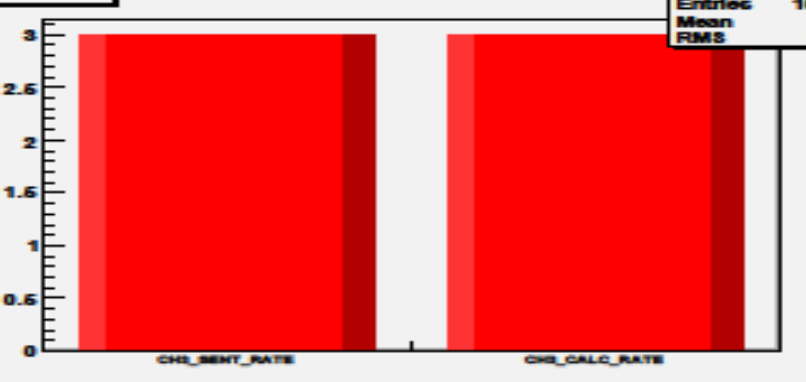
CH3_Oscillo



CH3_Oscillo

CH3_COUNTERS

CH3_COUNTERS



V. Conclusions & prospective:

-The CVD polycrystalline diamond based double sided strip detectors seems to be well suited to the requirements for a beam profiler for characterising low intensity radioactive heavy ion beams:

- material: ELP (small bulk polarization; signal stable in time); P2 from Company 1, for example
- thickness: 200-300 μ adequate for R~50 μ
- electric field ~1V/ μ ; HV though Sh < Se
- strip: 1 mm pitch (0.9mm strip, inter-strip gap: 0.1mm), efficiency: 90-99% (localization with 1 mm resolution)
- small cross-talk effects
- signal shape study: ~1.5 ns rise time for 1 strip; PSA may bring interesting information ($\Delta Q < \Delta V_{extrem}$)

-The further characterisation of such detectors and the engineering of the readout electronics and other associated elements of a fully fledged profiler are expected to be carried in the near future:

- tests for radiation hardness
- more robust electric contacts between PCB and strips?
- line receiver multi-channel preamplifiers for low energies
- acquisition system: FASTER + SCATS .
- Note: The study of the diamond detector has already been subject for a few student stages

SCATS (Sixteen Channel Absolute Time Stamper)
To be used by a new 50 X 50 diamond
BEAM PROFILER

References

- [1] E.-K. Souw, R.J. Meilunas, Nucl. Instr. And Meth. In Phys. Res. A 400 (1997) 69.
- [2] S. Schwertel et al., „Diamond detectors for the R3B Experiment”, GSI Scientific Report 2007 (GSI Report 2008-1), Instruments-Methods-10, (2007) 216.
- [3] P. Moritz, E. Bedermann, K. Blasche, H. Rodl, H. Stelzer, F. Zeytouni, DIPAC III, Frascati (1997).
- [4] J.-L. Lecouey et al., Abstract n°. 226, ANIMMA, Marseille (2009).
- [5] P. Bergonzo, D. Tromson, H. Hamrita, C. Mer, N. Tranchant, M. Nesladek, Diamond and Related Materials 16 (2007) 1038.
- [6] A. Brauning-Demian, E. Bedermann, P. Verma and P.H. Mokler, DIPAC III, Frascati (1997).

We are in collaboration with:

GSI (Darmstadt): Angela Bräuning-Demian, Elèni Berdermann, M. Traeger, M. Ciobanu & Detector Laboratory

LIST (CEA Saclay): Hassen Hamrita, Philippe Bergonzo

NIPNE Bucharest: Dana Dimitriu, Daniela Fluerasu

LPC Caen:

Jean-Marc Fontbone, Jérôme Perronnel, Hervé Plard, Jean-François Cam

Jean Hommet – acquisition; Yvan Merrer – mécanique + atelier mécanique

Lynda Achouri, Giacomo Randisi, Nigel Orr, Marian Pârlog

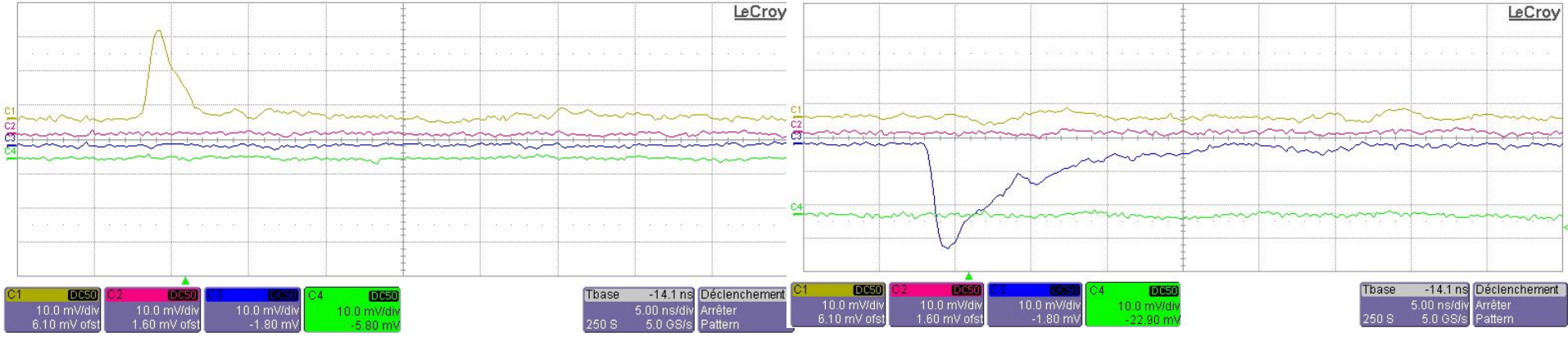
Remerciements:

Fac. Chimie: M. Ledauphin CRISMAT: Yohann Thimont, Séverine Mouchel

IPN Lyon: Michel Chevalier

CIMAP: Emmanuel Balanzat, Jean-Marc Ramillon, Stéphane Guillois

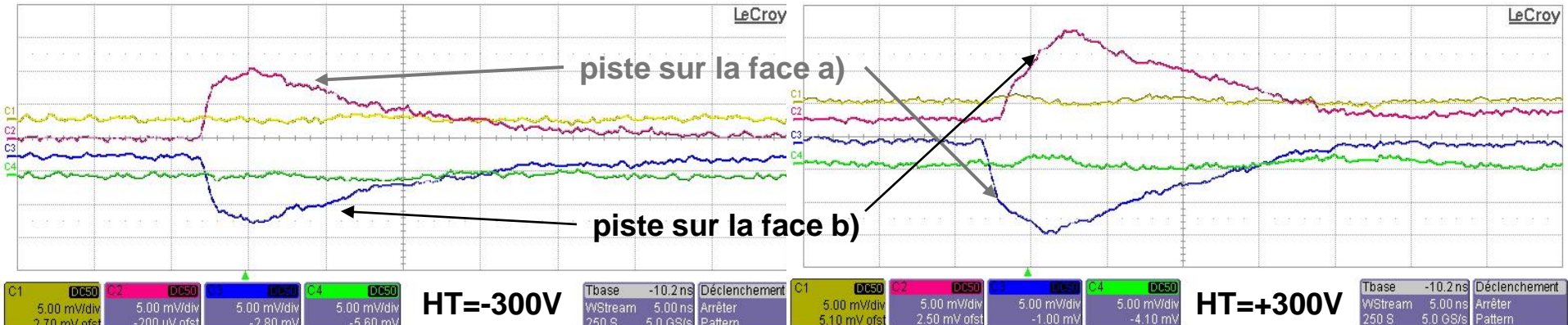
LPC: Joel Brégéault, Jean-Louis Gabriel, Albert Leconte, Christophe Vandamme, l'équipe informatique



Signals from the strip no. 9 of the face a) - left (yellow curve) and from the strip 9 of the face b) - right (blue curve), amplified with the new preamplifier PRL developed at LPC; the signals were induced by the ^{70}Zn ions of 8.7 AMeV in the detector IV of ELP type for a voltage of -300 V applied on the face a) (growth), irradiated

Signaux coincidentes sur les deux faces du détecteur

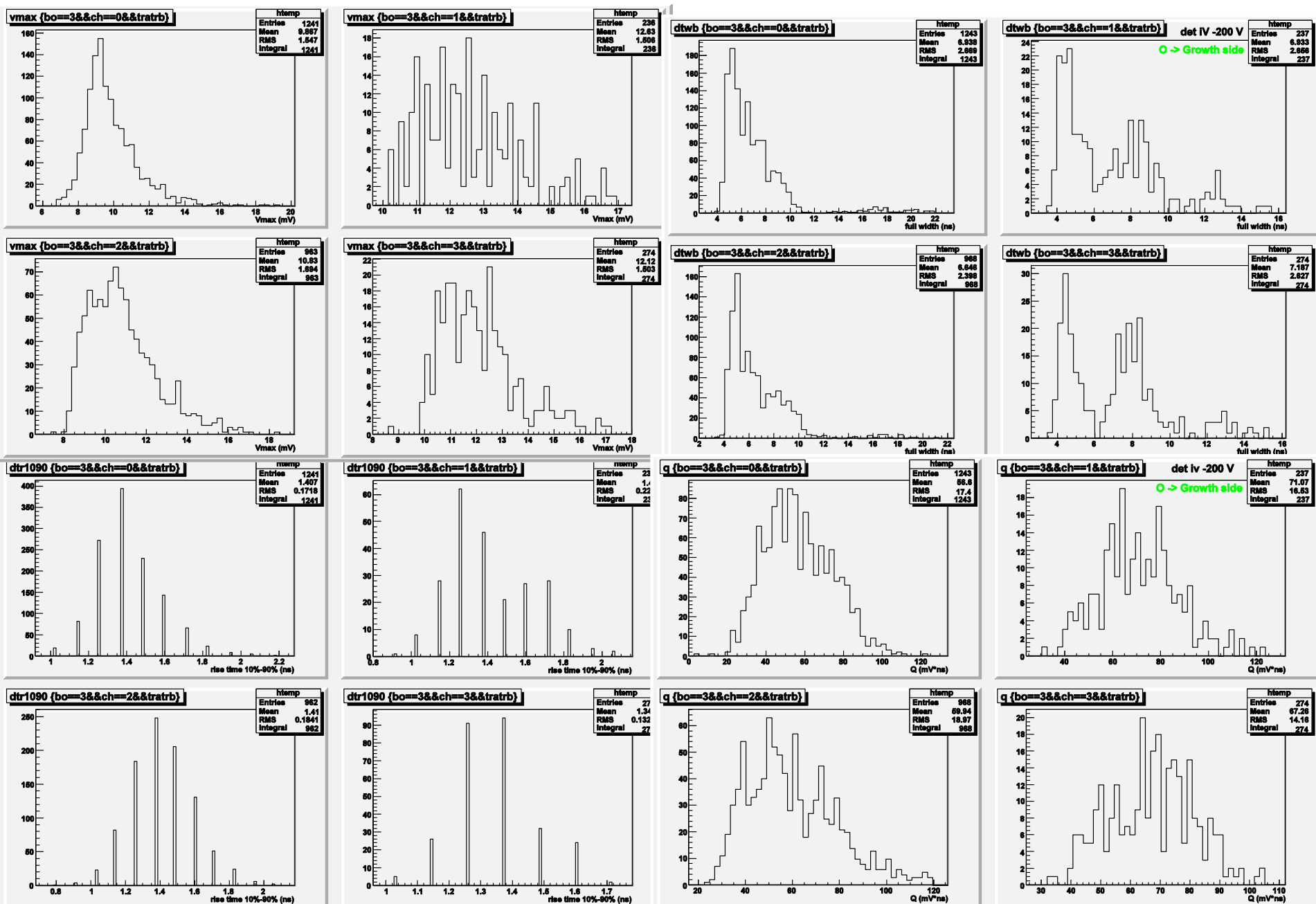
HT sur la face a) irradiée (1V/ μ)



Signals induced by ^{70}Zn of 8.7 AMeV in the detector IV of ELP type

Det iv ELP, 350 μ , -200 V, E=0.6V/ μ , board 3; O:13.7 AMeV

the 4 channels of Matacq board 3 give similar results



Det iv ELP, 350 μ -200 V, E=0.6V/ μ , board 3; O :13.7 AMeV

